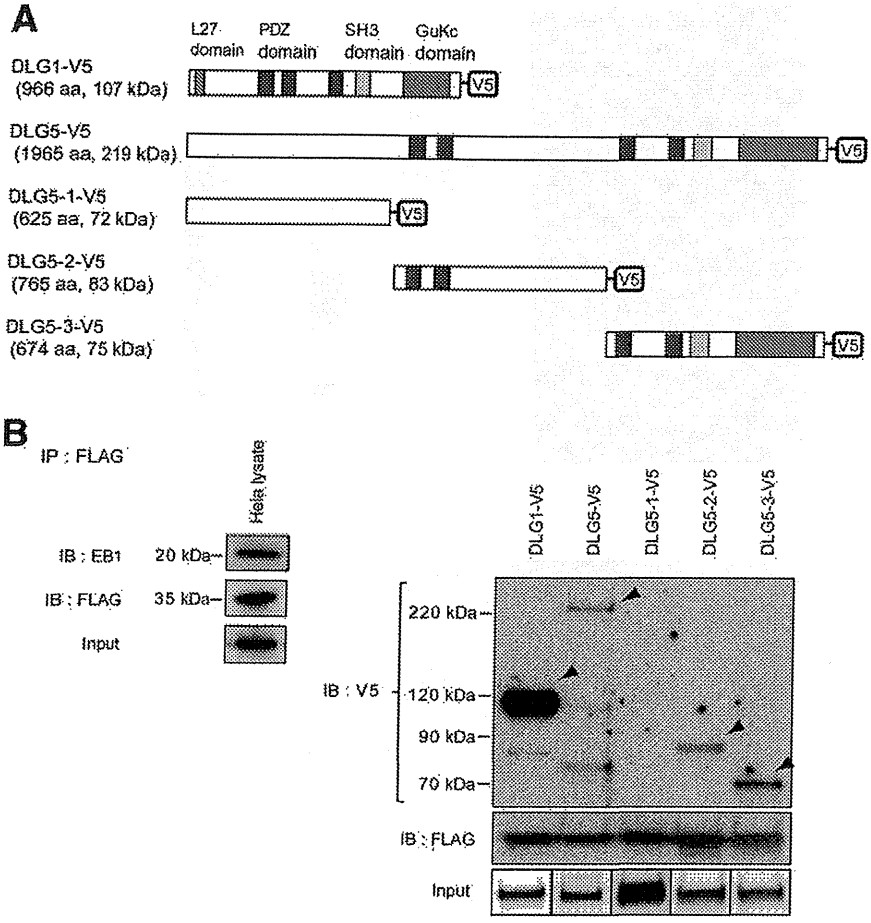

Figure 6 Association of the APC C terminus with EB1, DLG, and DLG5 *in vitro*. **A:** Domain structures and schematic representation of the DLG1 and DLG5 constructs encoding an N-terminal V5 epitope tag: DLG1-V5 (966 amino acids; 107 kDa), DLG5-V5 (1965 amino acids; 219 kDa), DLG5-1-V5 (625 amino acids; 72 kDa), DLG5-2-V5 (765 amino acids; 83 kDa), and DLG5-3-V5 (674 amino acids; 75 kDa). **B:** Binding of the EB1, DLG1, and DLG5 proteins to the FLAG-tagged C terminus of APC (FLAG-APC-C-term; 347 amino acids, 37 kDa) that is absent in the KAD rat. The FLAG-APC-C-term and each construct were co-transfected to Hela cells. The FLAG-APC-C-term was then immunoprecipitated by the FLAG antibody. Immunoprecipitated proteins were subjected to Western blotting to detect proteins that were co-immunoprecipitated with FLAG-APC-C-term. EB1 was detected using the anti-EB1 antibody. DLG1, DLG5, DLG5-1, DLG5-2, and DLG5-3 were detected using the anti-V5 antibody. EB1, DLG1, DLG5, DLG5-2, and DLG5-3 were co-immunoprecipitated with the FLAG-APC-C-term (**arrowheads**).

cytoskeleton. APC protein accumulated at the ends of the MTs at the migrating edges of both F344 and KAD rat VECs (Supplemental Figure S2). The incorporation of BrdU into KAD rat VECs was not different from that seen in F344 rat VECs (F344: 1.00 ± 0.04 versus KAD: 1.01 ± 0.03; $P = 0.92$). A wound healing assay demonstrated that the migration activity of KAD rat VECs stimulated with vascular endothelial growth factor was not different from that of F344 rat VECs (F344: 44.9 ± 6.03 versus KAD: 41.7 ± 7.30; $P = 0.11$).

A wash assay revealed significantly higher adhesion activity in KAD rat VECs than that in F344 rat VECs (Figure 5A). Immunostaining with antipaxillin antibody demonstrated that the number of focal adhesion sites of KAD rat VECs was significantly higher than that of F344 rat VECs (Figure 5, B and C). The capillary-like structure of KAD rat VECs induced on Matrigel revealed apparent differences in morphology compared with those of F344 rat VECs (Figure 5D). The length of tubes of KAD rat VECs was significantly shorter than that of F344 rat VECs (Figure 5E). The number of branches of KAD rat VECs was significantly fewer than that of F344 rat VECs (Figure 5F). These findings indicate that KAD rat VECs had normal physiologic function in morphology, proliferation, and migration but defects in adhesion and tube formation.

EB1 and DLG5 Could Bind to the C Terminus of APC and Are Expressed in the VECs of the Inflamed Colonic Region

To find molecules that interact with the C terminus of APC at the VEC in the inflamed area, we performed an Immunoprecipitation assay and fluorescent IHC. The C terminus of APC, which is absent in KAD rats, can interact with EB1 and DLG1.[12] Recently, DLG5 has been reported to be associated with pathogenesis of IBD.[27] Because DLG5 and DLG1 share the postsynaptic density protein-95/disks large/zonula occludens-1 (PDZ) domains that are known to bind to the C terminus of APC (Figure 6A) and the most characteristic feature of IBD is sustained inflammation of the colon, we examined whether DLG5, similar to EB1 and DLG1, can bind to the C terminus of APC.

Similar to EB1 and DLG1, full-length DLG5 was co-immunoprecipitated with the FLAG-APC-C-term (Figure 6B). Although we could not detect DLG5-1-V5, containing the first third of DLG5, we could detect DLG5-2-V5 and DLG5-3-V5, containing the second and final third of DLG5, respectively (Figure 6B). Both DLG5-2-V5 and DLG5-3-V5 contain PDZ domains, similar to DLG1, but the DLG-1-V5 contained no PDZ domain. Thus, these results indicate that the C terminus of APC could interact with the PDZ domain of DLG5.

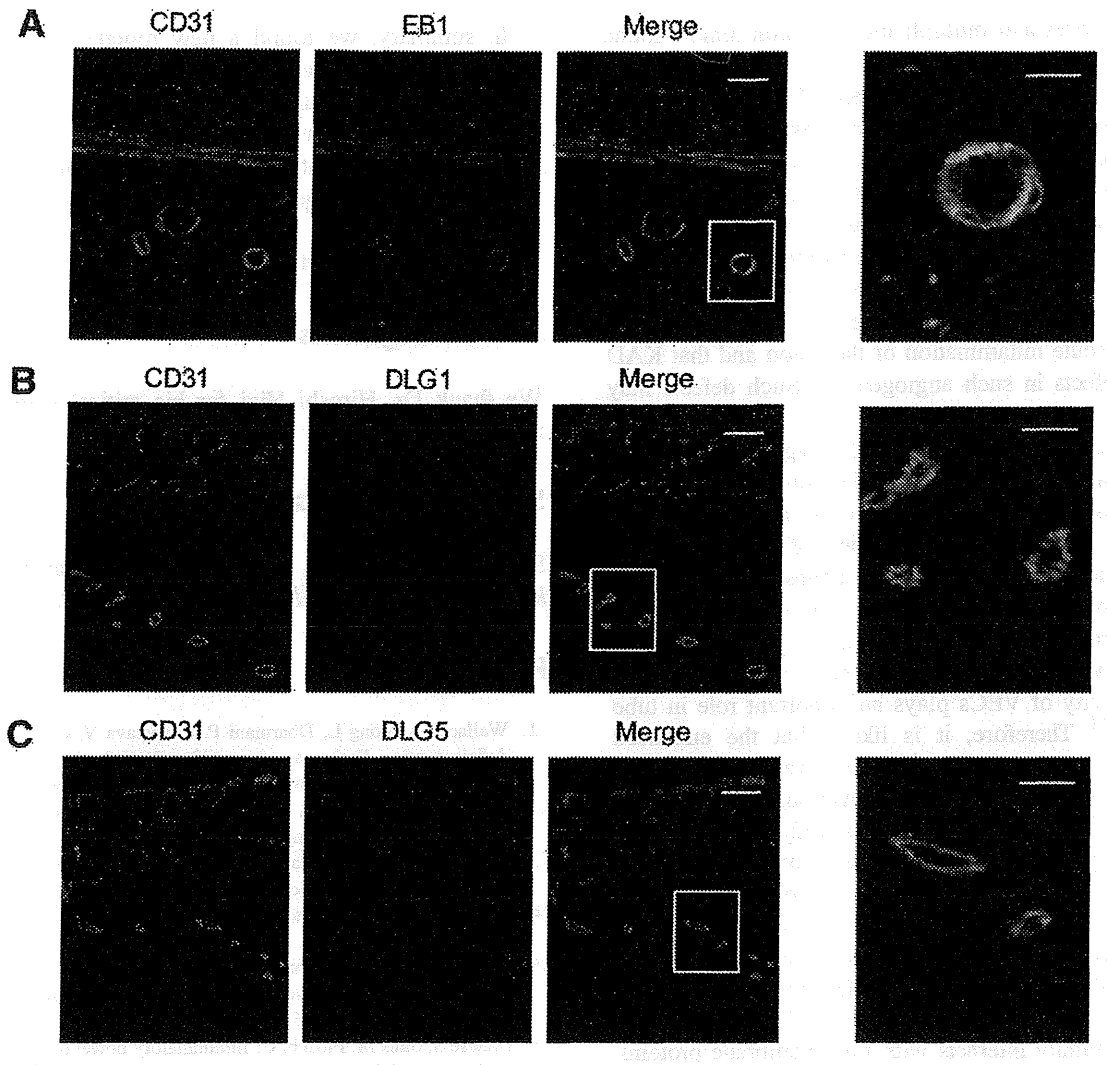

Figure 7 Localization of EB1 and DLG5 in the vascular endothelial cells of inflamed colon of F344 rats. Representative images of CD31 and EB1 (A), DLG1 (B) or DLG5 (C) co-fluorescent staining of distal colonic lesions from F344 rats immediately after DSS treatment (week 1). EB1 and DLG5, but not DLG1, were highly expressed in VECs at the submucosa. Scale bar = 50 μm. Images in the **right column** are magnified from the **boxed areas** of the merged images. Scale bar = 20 μm.

Fluorescent IHC analysis of inflamed colonic tissue at week 1, immediately after DSS treatment, revealed that EB1 and DLG5, but not DLG1, were expressed in the VECs (Figure 7). EB1 was also expressed in the severely ulcerated mucosal region (Figure 7A). DLG1, DLG5, and EB1 were not expressed in the VECs of the colon before the DSS treatment (data not shown). Thus, these findings indicate that the expression of EB1 and DLG5 was induced in VECs when colon inflammation occurred and that DLG5, rather than EB1, showed a pattern of expression similar to that of the APC protein (Figure 3).

Discussion

APC has been identified as the causative gene of the familial adenomatous polyposis of the colon. APC negatively regulates Wnt signaling by interacting with β-catenin via its β-catenin binding sites. Truncation of the APC protein at β-catenin binding sites result in the activation of Wnt signaling, which is a hallmark of the initiation of carcinogenesis in colonic epithelial cells.[12,28,29] In KAD rats (homozygous for the $Apc^{\Delta 2523}$ mutation), Wnt signaling is normal because the β-catenin binding sites are intact. Thus, we could exclude the effects of Wnt signaling when we compared physiologic characteristics found in KAD and control F344 rats. Alternatively, we could ascribe characteristic differences to the physiologic function of the C terminus of APC.

Even 3 weeks after terminating DSS treatment, KAD rats had continuous elevation of the expression of inflammatory-related genes, such as *Cox2* and *Ptges*, and enhanced cell proliferation, which were coincident with persistent inflammation. COX-2 and PTGES are functionally coupled for the biosynthesis of prostaglandin E2,[30] which plays a critical role during tumorigenesis in the gastrointestinal tract.[31,32] Thus, these findings can explain the significantly

higher incidences and multiplicities of colon tumors found in KAD rats compared with the control F344 rats.[16]

Immediately after DSS treatment, KAD rats had an abnormal deposition of fibrin in microvessels, instead of a normal formation of fibrin layers to cover the damaged mucosa. KAD rats also had decreased microvessel angiogenesis in the damaged colonic mucosa immediately after DSS treatment. Given the evident increase in expression of APC in VECs of the edematous submucosa, it is likely that APC has a critical role in angiogenesis that is driven in response to acute inflammation of the colon and that KAD rats have defects in such angiogenesis. Such defects may result in a delay in the repair process of the damaged mucosa possibly because of the shortage of oxygen and nutrition supply and therefore a persistence of colitis in KAD rats.

To determine how APC is involved in angiogenesis, we characterized the physiologic function of VECs of KAD rats. KAD rat VECs had stronger adhesion and formed abnormal tube morphology, which was characterized by a smaller number of branching points and a shorter length when VECs were stimulated to form tubes on Matrigel. The adhesion activity of VECs plays an important role in tube formation.[33,34] Therefore, it is likely that the enhanced adhesion activity may result in the low branched and short tubes found in KAD rat VECs. Although VECs were prepared from the thoracic aorta in this study, defects in tube formation may explain the decreased number of microvessels found in the damaged colonic mucosa of KAD rats.

Expression of both APC and DLG5 was specifically induced in the VEC of the inflamed colon at week 1, immediately after DSS treatment. DLG5 interacted with the C terminus of APC, probably via its PDZ domains. The DLG protein family interacts with transmembrane proteins in endothelial cells and is associated with angiogenesis.[35] Thus, we consider that the APC-DLG5 molecular pathway may function in the regulation of angiogenesis and cell adhesion of VECs.

It is known that abnormal angiogenesis contributes to the initiation and perpetuation of IBD and that microvessel dysfunction causes poor mucosal healing in IBD.[36,37] Similar to IBD patients, KAD rats had reduced angiogenesis in the inflamed mucosa and the KAD VECs had reduced adhesion activity. The human *DLG5* locus is associated with the pathogenesis of IBD.[27] In rats, expression of DLG5 can be induced by DSS treatment, and DLG5 binds to the C terminus of APC, which is absent in KAD rats. These results suggest that both APC and DLG5 may be involved in the pathogenesis of IBD. Further genetic analysis of relevant human populations may clarify the involvement of APC in the development of colitis.

It is expected that mutant APC derived from the $Apc^{\Delta 2523}$ allele may coexist with wild-type APC in the heterozygous KAD ($Apc^{\Delta 2523}/+$) rat because transcripts from the mutant allele can escape nonsense-mediated decay. Thus, further study using heterozygous rats may reveal dominant negative functions of the mutant APC.

In summary, we found a new function of APC in the pathogenesis of colonic inflammation, which appears to be mediated by the regulation of cellular adhesion activity of VECs. Molecular interaction of APC with DLG5 may function in the regulation of angiogenesis and cell adhesion of VECs. Our findings suggest that APC may contribute to the pathogenesis of IBD, in which patients are more susceptible to colorectal cancers.

Acknowledgments

We thank Dr. Hiroshi Hiai for his critical reading of the manuscript.

Supplemental Data

Supplemental material for this manuscript can be found at *http://dx.doi.org/10.1016/j.ajpath.2012.12.005*.

References

1. Wallace JL, Vong L, Dharmani P, Srivastava V, Chadee K: Muc-2-deficient mice display a sex-specific: COX-2-related impairment of gastric mucosal repair. Am J Pathol 2011, 178:1126–1133
2. Tonnesen MG, Feng X, Clark RA: Angiogenesis in wound healing. J Investig Dermatol Symp Proc 2000, 5:40–46
3. Tarnawski AS: Cellular and molecular mechanisms of gastrointestinal ulcer healing. Dig Dis Sci 2005, 50(Suppl 1):S24–S33
4. Podolsky DK: Inflammatory bowel disease. N Engl J Med 2002, 347: 417–429
5. Bernstein CN, Blanchard JF, Kliewer E, Wajda A: Cancer risk in patients with inflammatory bowel disease: a population-based study. Cancer 2001, 91:854–862
6. Danese S, Sans M, Fiocchi C: Inflammatory bowel disease: the role of environmental factors. Autoimmun Rev 2004, 3:394–400
7. Cooney R, Jewell D: The genetic basis of inflammatory bowel disease. Dig Dis 2009, 27:428–442
8. Kawada M, Arihiro A, Mizoguchi E: Insights from advances in research of chemically induced experimental models of human inflammatory bowel disease. World J Gastroenterol 2007, 13: 5581–5593
9. Okayasu I, Hatakeyama S, Yamada M, Ohkusa T, Inagaki Y, Nakaya R: A novel method in the induction of reliable experimental acute and chronic ulcerative colitis in mice. Gastroenterology 1990, 98: 694–702
10. Groden J, Thliveris A, Samowitz W, Carlson M, Gelbert L, Albertsen H, Joslyn G, Stevens J, Spirio L, Robertson M, Sargeant L, Krapcho K, Wolff E, Burt R, Hughes JP, Warrington J, McPherson J, Wasmuth J, Le Paslier D, Abderrahim H, Cohen D, Leppert M, White R: Identification and characterization of the familial adenomatous polyposis coli gene. Cell 1991, 66:589–600
11. Oshima M, Oshima H, Kitagawa K, Kobayashi M, Itakura C, Taketo M: Loss of Apc heterozygosity and abnormal tissue building in nascent intestinal polyps in mice carrying a truncated Apc gene. Proc Natl Acad Sci U S A 1995, 92:4482–4486
12. Aoki K, Taketo MM: Adenomatous polyposis coli (APC): a multifunctional tumor suppressor gene. J Cell Sci 2007, 120:3327–3335
13. Beroud C, Soussi T: APC gene: database of germline and somatic mutations in human tumors and cell lines. Nucleic Acids Res 1996, 24: 121–124
14. Smits R, Kielman MF, Breukel C, Zurcher C, Neufeld K, Jagmohan-Changur S, Hofland N, van Dijk J, White R, Edelmann W,

Kucherlapati R, Khan PM, Fodde R: Apc1638T: a mouse model delineating critical domains of the adenomatous polyposis coli protein involved in tumorigenesis and development. Genes Dev 1999, 13: 1309–1321
15. Yokoyama A, Nomura R, Kurosumi M, Shimomura A, Onouchi T, Iizuka-Kogo A, Smits R, Oda N, Fodde R, Itoh M, Senda T: The C-terminal domain of the adenomatous polyposis coli (Apc) protein is involved in thyroid morphogenesis and function. Med Mol Morphol 2011, 44:207–212
16. Yoshimi K, Tanaka T, Takizawa A, Kato M, Hirabayashi M, Mashimo T, Serikawa T, Kuramoto T: Enhanced colitis-associated colon carcinogenesis in a novel Apc mutant rat. Cancer Sci 2009, 100:2022–2027
17. Yoshimi K, Hashimoto T, Niwa Y, Hata K, Serikawa T, Tanaka T, Kuramoto T: Use of a chemically induced-colon carcinogenesis-prone Apc-mutant rat in a chemotherapeutic bioassay. BMC Cancer 2012, 12:448
18. Melgar S, Karlsson A, Michaelsson E: Acute colitis induced by dextran sulfate sodium progresses to chronicity in C57BL/6 but not in BALB/c mice: correlation between symptoms and inflammation. Am J Physiol Gastrointest Liver Physiol 2005, 288:G1328–G1338
19. Vermeulen PB, Gasparini G, Fox SB, Toi M, Martin L, McCulloch P, Pezzella F, Viale G, Weidner N, Harris AL, Dirix LY: Quantification of angiogenesis in solid human tumours: an international consensus on the methodology and criteria of evaluation. Eur J Cancer 1996, 32A: 2474–2484
20. Feroze-Merzoug F, Berquin IM, Dey J, Chen YQ: Peptidylprolyl isomerase A (PPIA) as a preferred internal control over GAPDH and beta-actin in quantitative RNA analyses. Biotechniques 2002, 32: 776–778, 780, 782
21. Shi W, Wang NJ, Shih DM, Sun VZ, Wang X, Lusis AJ: Determinants of atherosclerosis susceptibility in the C3H and C57BL/6 mouse model: evidence for involvement of endothelial cells but not blood cells or cholesterol metabolism. Circ Res 2000, 86:1078–1084
22. Kroboth K, Newton IP, Kita K, Dikovskaya D, Zumbrunn J, Waterman-Storer CM, Nathke IS: Lack of adenomatous polyposis coli protein correlates with a decrease in cell migration and overall changes in microtubule stability. Mol Biol Cell 2007, 18:910–918
23. Matsumoto S, Fumoto K, Okamoto T, Kaibuchi K, Kikuchi A: Binding of APC and dishevelled mediates Wnt5a-regulated focal adhesion dynamics in migrating cells. EMBO J 2010, 29:1192–1204
24. Shimizu T, Suzuki M, Fujimura J, Hisada K, Yoshikazu O, Obinata K, Yamashiro Y: The relationship between the concentration of dextran sodium sulfate and the degree of induced experimental colitis in weanling rats. J Pediatr Gastroenterol Nutr 2003, 37:481–486
25. Ingber DE: Mechanical signaling and the cellular response to extracellular matrix in angiogenesis and cardiovascular physiology. Circ Res 2002, 91:877–887
26. Li D, Xie S, Ren Y, Huo L, Gao J, Cui D, Liu M, Zhou J: Microtubule-associated deacetylase HDAC6 promotes angiogenesis by regulating cell migration in an EB1-dependent manner. Protein Cell 2011, 2: 150–160
27. McGovern DP, Gardet A, Torkvist L, Goyette P, Essers J, Taylor KD, Neale BM, Ong RT, Lagace C, Li C, Green T, Stevens CR, Beauchamp C, Fleshner PR, Carlson M, D'Amato M, Halfvarson J, Hibberd ML, Lordal M, Padyukov L, Andriulli A, Colombo E, Latiano A, Palmieri O, Bernard EJ, Deslandres C, Hommes DW, de Jong DJ, Stokkers PC, Weersma RK, Sharma Y, Silverberg MS, Cho JH, Wu J, Roeder K, Brant SR, Schumm LP, Duerr RH, Dubinsky MC, Glazer NL, Haritunians T, Ippoliti A, Melmed GY, Siscovick DS, Vasiliauskas EA, Targan SR, Annese V, Wijmenga C, Pettersson S, Rotter JI, Xavier RJ, Daly MJ, Rioux JD, Seielstad M: Genome-wide association identifies multiple ulcerative colitis susceptibility loci. Nat Genet 2010, 42:332–337
28. Akiyama T, Kawasaki Y: Wnt signalling and the actin cytoskeleton. Oncogene 2006, 25:7538–7544
29. Senda T, Iizuka-Kogo A, Onouchi T, Shimomura A: Adenomatous polyposis coli (APC) plays multiple roles in the intestinal and colorectal epithelia. Med Mol Morphol 2007, 40:68–81
30. Murakami M, Naraba H, Tanioka T, Semmyo N, Nakatani Y, Kojima F, Ikeda T, Fueki M, Ueno A, Oh S, Kudo I: Regulation of prostaglandin E2 biosynthesis by inducible membrane-associated prostaglandin E2 synthase that acts in concert with cyclooxygenase-2. J Biol Chem 2000, 275:32783–32792
31. Oshima M, Dinchuk JE, Kargman SL, Oshima H, Hancock B, Kwong E, Trzaskos JM, Evans JF, Taketo MM: Suppression of intestinal polyposis in $Apc^{\Delta 716}$ knockout mice by inhibition of cyclooxygenase 2 (COX-2). Cell 1996, 87:803–809
32. Sonoshita M, Takaku K, Sasaki N, Sugimoto Y, Ushikubi F, Narumiya S, Oshima M, Taketo MM: Acceleration of intestinal polyposis through prostaglandin receptor EP2 in $Apc^{\Delta 716}$ knockout mice. Nat Med 2001, 7:1048–1051
33. Drake CJ, Hungerford JE, Little CD: Morphogenesis of the first blood vessels. Ann N Y Acad Sci 1998, 857:155–179
34. Davis GE, Stratman AN, Sacharidou A, Koh W: Molecular basis for endothelial lumen formation and tubulogenesis during vasculogenesis and angiogenic sprouting. Int Rev Cell Mol Biol 2011, 288: 101–165
35. Yamamoto Y, Irie K, Asada M, Mino A, Mandai K, Takai Y: Direct binding of the human homologue of the Drosophila disc large tumor suppressor gene to seven-pass transmembrane proteins, tumor endothelial marker 5 (TEM5), and a novel TEM5-like protein. Oncogene 2004, 23:3889–3897
36. Koutroubakis IE, Tsiolakidou G, Karmiris K, Kouroumalis EA: Role of angiogenesis in inflammatory bowel disease. Inflamm Bowel Dis 2006, 12:515–523
37. Papa A, Scaldaferri F, Danese S, Guglielmo S, Roberto I, Bonizzi M, Mocci G, Felice C, Ricci C, Andrisani G, Fedeli G, Gasbarrini G, Gasbarrini A: Vascular involvement in inflammatory bowel disease: pathogenesis and clinical aspects. Dig Dis 2008, 26:149–155

Carcinogenesis vol.34 no.2 pp.361–369, 2013
doi:10.1093/carcin/bgs348
Advance Access publication November 3, 2012

Organomagnesium suppresses inflammation-associated colon carcinogenesis in male Crj: CD-1 mice

Toshiya Kuno[1], Yuichiro Hatano[1], Hiroyuki Tomita[1], Akira Hara[1], Yoshinobu Hirose[1], Akihiro Hirata[2], Hideki Mori[1], Masaru Terasaki[3], Sonoko Masuda[3] and Takuji Tanaka[1,4,*]

[1]Department of Tumor Pathology, Gifu University Graduate School of Medicine, 1-1 Yanagido, Gifu 501–1194, Japan, [2]Division of Animal Experiment, Life Science Research Center, Gifu University Graduate School of Medicine, 1-1 Yanagido, Gifu 501–1194, Japan, [3]Department of Health and Environmental Sciences, Faculty of Pharmaceutical Sciences, Health Sciences University of Hokkaido, 1757 Kanazawa, Ishikari-Tobetsu, Hokkaido 061-0293, Japan and [4]The Tohkai Cytopathology Institute: Cancer Research and Prevention (TCI-CaRP), 5-1-2 Minami-uzura, Gifu City, Gifu 500–8285, Japan

*To whom correspondence should be addressed. Tel: +81 58 273 4399; Fax: +81 58 273 4392;
Email: takutt@toukaisaibou.co.jp

Magnesium (Mg) deficiency increases genomic instability and Mg intake has been reported to be inversely associated with a risk of colorectal cancer (CRC). This study was designed to determine whether organo-Mg in drinking water suppresses inflammation-associated colon carcinogenesis in mice. Male Crj: CD-1 mice were initiated with a single i.p. injection of azoxymethane (AOM, 10 mg/kg body weight) and followed by a 1 week exposure to dextran sulfate sodium (DSS, 1.5%, w/v) in drinking water to induce colonic neoplasms. They were then given the drinking water containing 7, 35 or 175 p.p.m. organo-Mg for 13 weeks. The chemopreventive efficacy of organo-Mg was determined 16 weeks after the AOM exposure. Administration with organo-Mg at all doses caused a significant inhibition of CRC development ($P < 0.01$ and $P < 0.001$). Especially, the highest dose of organo-Mg significantly suppressed the occurrence of all the colonic pathological lesions (mucosal ulcer, dysplasia, adenoma and adenocarcinoma). Organo-Mg also significantly reduced the number of mitoses/anaphase bridging, as well as proliferation of CRC. Additionally, at week 4, organo-Mg lowered the messenger RNA expression of certain proinflammatory cytokines, such as interleukin-1β, interleukin-6, interferon-γ and inducible nitric oxide synthase in the lesion-free colorectal mucosa at week 4 but increased the Nrf-2 messenger RNA expression. Our findings that organo-Mg inhibits inflammation-related mouse colon carcinogenesis by modulating the proliferative activities and chromosomal instability of CRC and suppressing colonic inflammation may suggest potential use of organo-Mg for clinical chemoprevention trials of CRC in the inflamed colon.

Introduction

Cancer incidence in the developed countries has increased throughout this century and has already been the leading cause of death in some Western countries (1,2). Despite great advances in the integration of therapies for malignant epithelial malignancies, the 5-year survival rate for individuals with malignancies is still low. There has been a marked increase in the understanding of cell and molecular mechanisms underlying a variety of carcinogenic processes. However, therapeutic options for advanced neoplastic disease remain limited. This lack of treatment alternatives may be due to the large number of genetic and molecular alterations associated with advanced malignancies that contribute to the maintenance of neoplastic progression. Colorectal cancer (CRC) is the third-most common malignancy and the fourth-most common cause of cancer mortality worldwide (3). The chemopreventive approach to inhibit cancer development and progression is highly attractive. Practical limitations may exist with respect to developing novel and effective chemopreventive agents through the use of appropriate animal models for preclinical evaluation of candidate chemopreventive agents.

Magnesium (Mg) is an essential mineral rich in wheat germ, green vegetables, legumes, algae, nuts and seeds, which acts as a cofactor in enzymatic reactions in the human body. Meat, fruit and dairy products have moderate Mg content, whereas refined foods are poor sources of Mg. A large number of studies indicate that a higher consumption of Mg may favorably affect a cluster of metabolic and inflammatory disorders including insulin resistance (4), hypertension (5), dyslipidemia (6), diabetes mellitus (7), metabolic syndrome (6) and cardiovascular disease (5). Epidemiological studies have indicated an inverse association between dietary intake of Mg and incidence of certain types of cancer, including CRC (8,9). We previously reported that magnesium hydroxide in diet significantly suppressed colon carcinogenesis induced by azoxymetheane (AOM) in rats (10) by modulating cell proliferation activity of cryptal cells that was initiated with colonic carcinogens (11).

Patients with two major types of inflammatory bowel disease, ulcerative colitis (UC) and Crohn's disease, are at an increased risk for the development of CRC (12). Unlike sporadic CRC, CRC in UC patients arises from a focal or multifocal dysplastic mucosa in areas of inflammation (12). Chromosomal instability is frequently observed in chronic inflammatory conditions including UC by estimating aneuploidy (13,14). Inflammatory bowel disease–related CRC has also high rate of chromosomal instability when compared with sporadic CRC (15,16). Low Mg promotes oxidative stress and inflammation (17), which generate genetic instability and increases the risk of mutations (18). Inflammation is involved not only in the early stages of tumorigenesis but also in the late events since inflammatory mediators promote invasion and metastasis (18). Tumor necrosis factor (TNF)-α, interleukin (IL)-1 and IL-6 were induced under Mg deprivation (17).

The current study was designed to explore the possible cancer chemopreventive efficacy of Mg. We investigated the effects of Mg in drinking water on large bowel oncogenesis using an AOM/dextran sodium sulfate (DSS)–treated mouse model, which is a useful animal model to study chemoprevention in inflammation-related colon carcinogenesis (19,20). To understand the mechanism(s) by which organo-Mg modify AOM/DSS-induced colon carcinogenesis, expressions of inflammatory enzymes, such as COX-2, inducible nitric oxide synthase (iNOS) and inflammatory cytokines, such as TNF-α, IL-1β, IL-6 and interferon (IFN)-γ in the non-lesional colonic mucosa were examined. Since nuclear factor erythroid 2–related factor 2 (Nrf2), a transcriptional regulator of oxidant responses, expression and activation, plays a critical role in protecting colitis-associated CRC (21–23), mRNA expression of Nrf2 was assessed in colon mucosa. In addition, we determined whether organo-Mg in drinking water affects the chromosomal instability of adenocarcinoma cells by counting the number of anaphase-bridging formations (24,25). Effects of organo-Mg on growth of human colorectal adenocarcinoma cell line, DLD-1, were also evaluated.

Abbreviations: ABI, anaphase bridging index; AOM, azoxymetheane; CIN, chromosomal instability; CRC, colorectal cancer; DSS, dextran sulfate sodium; IL, interleukin; INF, interferon; iNOS, inducible nitric oxide synthase; Mg, magnesium; MCM2, minichromosome maintenance protein 2; Nrf2, nuclear factor erythroid 2–related factor 2; TNF, tumor necrosis factor; UC, ulcerative colitis.

Materials and methods

Chemicals

Organo-Mg was prepared by mixing magnesium oxide (0.22 g), citric acid (0.55 g), malic acid (0.55 g) and glycine (0.22 g) in the Tateho Chemical Industries Co., Ltd. (Ako City, Hyogo, Japan). X-ray diffraction of organo-Mg was performed in the Air Water Inc. (Sapporo, Japan). Organo-Mg (1.54 g) contained 132 mg Mg. AOM was purchased from Sigma-Aldrich Chemical Co. (St. Louis, MO, USA). DSS with a molecular weight of 36 000–50 000 was obtained from MP Biomedecals, LLC (Aurora, OH, USA). DSS 1.5% (w/v) was prepared just before use to induce colitis.

Animals

Five week old male Crj:CD-1 (ICR) mice were purchased from Japan SLC, Inc. All animals were housed in plastic cages (3–5 mice/cage) and had free access to tap water and a basal diet, CE-2 (CLEA Japan, Inc., Tokyo, Japan). The animals were kept in an experimental animal room under controlled conditions of humidity (50 ± 10%), light (12/12 h light/dark cycle) and temperature (23 ± 2°C). After 7 days of quarantine, animals were divided into five experimental groups and one control group. Experimental drinking water was prepared by dissolving organo-Mg in distilled water at three dose levels of 7, 35 and 175 p.p.m.

Animal experiment

The experimental and study design were approved by the Committee of Gifu University Animal Facility under the Institutional Animal Care guideline. All handling and procedures were carried out in accordance with the appropriate Institutional Animal Care Guidelines.

A total of 105 male ICR (4 weeks old) mice were divided into five experimental groups and one control group. Mice in groups 1 ($n = 21$), 2 ($n = 20$), 3 ($n = 21$) and 4 ($n = 20$) were given a single i.p. injection of AOM (10 mg/kg body weight). Beginning 7 days after the AOM injection, they also received 1.5% (w/v) DSS in drinking water for 7 days. Beginning 1 week following the final DSS exposure, the mice in groups 2–4 were given an experimental drinking water containing organo-Mg at doses of 7, 35 and 175 p.p.m. for 13 weeks, respectively. The mice in group 5 ($n = 11$) received only the 175 p.p.m. Mg-containing drinking water for 13 weeks. The mice of group 6 ($n = 12$) served as untreated controls. All groups were fed the basal diet CE-2 (CLEA Japna, Inc.) during the study.

At week 4, five mice each from each group were randomly selected and killed to measure mRNA expression target inflammatory enzymes and cytokines in the colonic mucosa by quantitative reverse transcription–PCR (RT–PCR). On killing, the large bowel of each animal was removed, the contents (feces) were washed out by physiologic saline and the length from the ileocecal junction to the anal verge was measured. After the large bowels were cut open longitudinally along the main axis and gently washed with saline, scraped colonic mucosa tissue was dipped into the RNAlater solution (Applied Biosystems/Ambion, Life Technologies Japan, Ltd., Tokyo, Japan). At week 16, all of the remaining animals were euthanized by exsanguinations through the abdominal aorta under isoflurane anesthesia and subjected to a complete gross necropsy examination to determine the incidence and multiplicity of tumors in the large bowel. At sacrifice, the large bowel was removed and the length was measured. Each large bowel was cut open longitudinally along the main axis and gently washed with saline, then examined manually to determine the incidence and multiplicity of tumors. The colon was fixed in 10% buffered formalin for at least 24 h. Histopathologic examination was done on hematoxylin and eosin–stained sections made from paraffin-embedded blocks. Colonic tumors were diagnosed according to criteria established in a prior study (19). The number and density of mucosal ulcers on hematoxylin and eosin–stained sections was also recorded.

Colitis was graded according to the following morphological criteria (26): showing normal appearance (grade 0); shortening and loss of the basal one-third of the actual crypts with mild inflammation in the mucosa (grade 1); loss of the basal two-thirds of the crypts with moderate inflammation in the mucosa (grade 2); loss of the entire crypts with severe inflammation in the mucosa and submucosa but with retainment of the surface epithelium (grade 3) and presence of mucosal ulcer with severe inflammation (neutrophils, lymphocytes, macrophages and plasma cells infiltration) in the mucosa, submucosa, muscularis propria and/or subserosa (grade 4). The scoring of inflammation was made on the entire colon with or without proliferative lesions and expressed as mean average score/mouse.

Immunohistochemical assessment of cell proliferation

Immunohistochemical analysis for the minichromosome maintenance protein 2 (MCM2) in the colon with or without tumors was done on 4 μm thick paraffin-embedded sections by the labeled avidin–biotin peroxidase complex method using a Vectastain ABC kit (Vector Laboratories Ltd., Burlingame, CA, USA), with microwave accentuation. Since MCM2 staining is a reliable marker of cell proliferation in colon cancer (27), we chose MCM2 to immunobistochemical assessment of proliferation of adenocarcimas in this study. The paraffin-embedded sections were heated for 30 min at 65°C, deparaffinized in xylene and rehydrated with ethanol at room temperature. Phosphate-buffered saline (pH 7.4; 0.01 mol/l) was used to prepare the solutions and for washes between the preparation steps. Incubations were done in a humidified chamber. The sections were treated for 40 min at room temperature with mouse IgG blocking reagent (Vector Laboratories Ltd.) and incubated overnight at 4°C with the primary antibody (1:400 dilution; MCM2 (D7G11) XPTM Rabbit monoclonal antibody, Cat. no., #3619, Cell Signaling Technology, Inc., Danvers, MA, USA). The antibody was applied to the sections according to the manufacturer's protocol. Horseradish peroxidase activity was visualized by treatment with H_2O_2 (DAKO Japan, Co., Ltd., Kyoto, Japan) and 3,3′-diaminobenzidine (DAKO Japan) for 5 min. In the last step, the sections were weakly counterstained with Mayer's hematoxylin (Merck). For each examination, negative controls were done on serial sections. The numbers of nuclei with positive reactivity for MCM2-immunohistochemistry were counted by two observers (T.T. and T.K.) who were unaware of the treatment groups to which the slides belonged. The positive rates were evaluated in >100 cancer cells each of 15 different areas of the adenocarcinomas from five mice each from groups 1–4 and expressed as percentage [mean ± standard deviation (SD)].

Mitotic index and anaphase bridging index of adenocarcinoma cells

To examine the effects of organo-Mg in drinking water on chromosomal instability (24,25) in adenocarcinoma cells, the anaphase bridging index (ABI) was determined on hematoxylin and eosin–stained sections. The numbers of mitoses and anaphase bridging were counted in >100 cancer cells from five adenocarcinomas each from groups 1 through 4. The mitotic index (MI; number of mitoses per cancer cells) and ABI (number of anaphases with bridging per mitoses) were expressed as percentages (mean ± SD).

Total RNA extraction and quantitative real-time RT–PCR

Total RNA was extracted from colonic mucosa using the RNeasy Mini Kit (Qiagen, Tokyo, Japan) according to the manufacturer's protocol. The complementary DNA was then synthesized from total RNA (0.2 μg) using the High-Capacity cDNA Reverse Transcription Kit (Applied Biosystems Japan Ltd., Tokyo, Japan). Quantitative real-time PCR analysis of individual complementary DNA was performed with ABI Prism 7500 (Applied Biosystems Japan Ltd.) using TaqMan Gene Expression Assays (Applied Biosystems Japan Ltd.; TNF-α, Mm00443258_m1; IL-1β, Mm00434228_m1; IL-6, Mm00446190_m1; INF-γ, Mm00801778_m1; COX-2 (Ptgs2), Mm00478374_m1; iNOS (Nos2), Mm00440485_m1 and β-actin: Mm00607939_s1). The sense and antisense primers Nrf2 mRNA were 5′-TTGGCAGACATTCCCAT-3′ and 5′-GCTGCCACCGTCACTGGG-3′, respectively. PCR cycling conditions were 50°C for 2 min, 95°C for 10 min, followed by 40 cycles of 95°C for 15 s and 60°C for 1 min. The expression level of each gene was normalized to the β-actin expression level using the standard curve method. Each assay was performed triplicate and the average was calculated.

Effects of organo-Mg on the growth of human colorectal adenocarcinoma cell line DLD-1

DLD-1 human colorectal cancer cells were purchased from American Type Culture Collection (Manassas, VA, USA). The cells were cultured in Dulbecco's modified Eagle's medium supplemented with 10% heat-inactivated fetal bovine serum. Fetal bovine serum and charcoal-dextran stripped fetal bovine serum were purchased from Biowest (Ringmer, UK). WST-1 reagent was obtained from Roche Diagnostics (Mannheim, Germany). The cells were cultured at 37°C in a humidified atmosphere of 95% air and 5% CO_2. Cell proliferation was estimated by WST-1 assay. DLD-1 cells were trypsinized, seeded at a density of 5×10^4 cells/ml 10% charcoal-dextran stripped fetal bovine serum /Dulbecco's modified Eagle's medium into 12-well plates and incubated for 6 h. Organo-Mg was dissolved in 1% charcoal-dextran stripped fetal bovine serum /Dulbecco's modified Eagle's medium, filtered at 0.2 μm of cellulose acetate and diluted from 1000 to 0 μg/ml. The cells were reintroduced to each concentration of medium containing organo-Mg. After 72 h incubation, WST-1 reagent was added to the medium and the cell viability was measured at 450 nm using plate reader.

Statistical analysis

Where applicable, data were analyzed using Fisher's exact probability test or one-way analysis of variance with Tukey's multiple comparisons test with $P < 0.05$ as the limit for statistical significance. Data on mRNA expression (mean ± SD) were analyzed by Kruskal–Wallis test.

Results

General observation

All animals remained healthy throughout the experimental period. The body weight gains by mice in all of the six groups were similar

Table I. Body weights and intakes of drinking water

Group no.	Treatment	Body weight (g)		Water consumption (ml/mouse/day)
		Initial (No. of mice)	Final (No. of mice)	
1	AOM/DSS	24.9±1.0[a] (21)	43.8±3.1 (16)	7.40±0.98
2	AOM/DSS/7 p.p.m. organo-Mg	24.8±1.0 (20)	47.6±5.8 (15)	7.76±0.57
3	AOM/DSS/35 p.p.m. organo-Mg	25.0±0.9 (21)	47.5±4.2 (16)	7.75±1.02
4	AOM/DSS/175 p.p.m. organo-Mg	24.8±1.1 (20)	46.9±4.6 (15)	7.05±0.60
5	175 p.p.m. organo-Mg	24.1±0.5 (11)	44.3±4.1 (6)	6.83±0.60
6	None	24.9±0.8 (12)	45.9±3.4 (7)	6.64±1.06

[a]Mean ± SD.

during the study. Food consumption (grams/day/mouse) did not differ significantly among the groups (data not shown). Also, the mean daily intake of drinking water with or without DSS did not significantly differ among the groups (Table I). The mean body weight at the termination (week 20) was not different among the groups (Table I). The mean colon length of group 1 was slightly shorter than that of other groups (data not shown) but it was not statistically significant.

Incidence and multiplicity of colonic lesions

Macroscopic colonic lesions, including tumors and small ulcerations, were seen in the mice in groups 1 through 4 (Figure 1). The mice of groups 5 and 6 did not develop colonic tumors (Figure 1).

Microscopic examinations revealed various pathologic colonic lesions in mice belonging to groups 1–4. The lesions included mucosal ulcers (Figure 2A), low- and high-grade dysplastic crypts (Figurer 2B), tubular adenomas (Figure 2C) and tubular adenocarcinomas with invasion (Figure 2D). Table II summarizes the microscopic data on the incidence and multiplicity of colonic lesions. The mean numbers of mucosal ulcers in groups 3 ($P < 0.05$) and 4 ($P < 0.01$) were also significantly smaller than that of group 1. Similarly, the mean numbers of high-grade dysplastic crypts in groups 3 ($P < 0.05$) and 4 ($P < 0.01$) were significantly lower than that of group 1. In additon, organo-Mg exposure to mice at 175 p.p.m. in the drinking water significantly diminished the incidences of colorectal adenoma and adenocarcinoma ($P < 0.01$ for both the lesions). The administration of 7 p.p.m. organo-Mg (group 2) significantly reduced the multiplicity ($P < 0.01$) of adenocarcinomas and the number of total tumors (adenoma + adenocarcinoma, $P < 0.01$) when compared with group 1. Drinking with 35 p.p.m. organo-Mg (group 3) also significantly lowered the numbers of adenocarcinomas and total tumors when compared with group 1 ($P < 0.01$ for each comparison). Furthermore, intake of 175 p.p.m. organo-Mg (group 4) significantly lowered the numbers of adenomas, adenocarcinomas and total tumors ($P < 0.001$ for each comparison) when compared with group 1.

Scores of inflammation in the colorectum

As illustrated in Figure 3, AOM and DSS treatment induced colitis with an inflammation score 2.06±0.93. Administration with organo-Mg in drinking water significantly lowered the score of inflammation in the colorectum at 7 p.p.m. ($P < 0.05$), 35 p.p.m. ($P < 0.001$) and 175 p.p.m. ($P < 0.001$). The inflammation score of the organo-Mg (175 p.p.m.) alone group was comparable with that of the untreated group.

MCM2-positive indices of adenocarcinomas

The data on the proliferative kinetics in the colonic adenocarcinomas by estimating the MCM2-positive indices are shown in Figure 4. The MCM2-positive indices for colonic adenocarcinomas in groups 2 (48.9±20.0, $P < 0.001$), 3 (40.5±16.4, $P < 0.001$) and 4 (28.6±8.4, $P < 0.001$) were significantly lower than in group 1 (65.0±13.9).

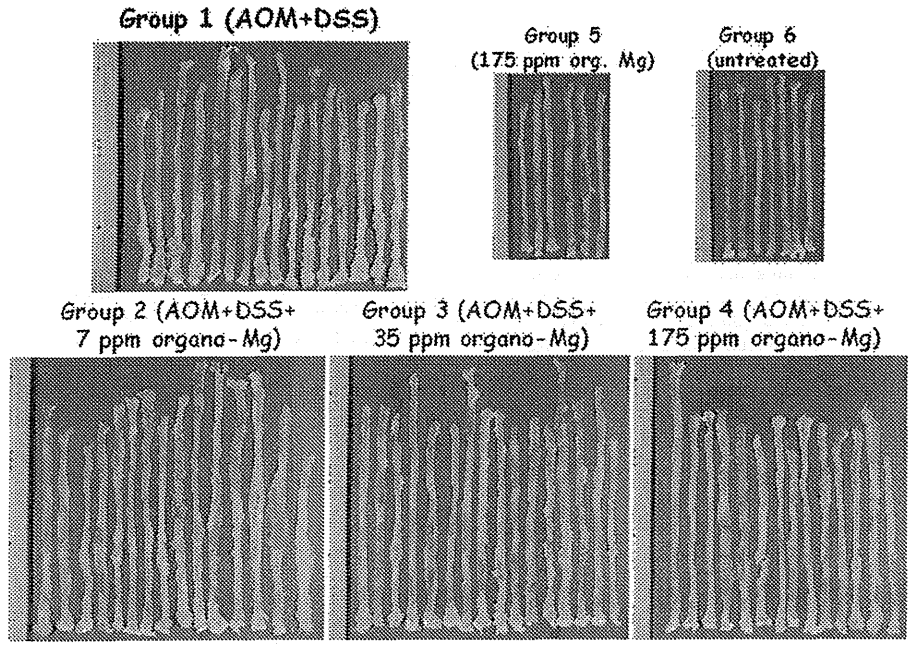

Fig. 1. Macroscopic views of the colon from the mice of groups 1–6 at the end of the study. Many tumors developed in the colon of mice in group 1 but number of colon tumors in groups 2–4 were less when compared with group 1. There were no tumor developed in the colon of mice in groups 5 and 6.

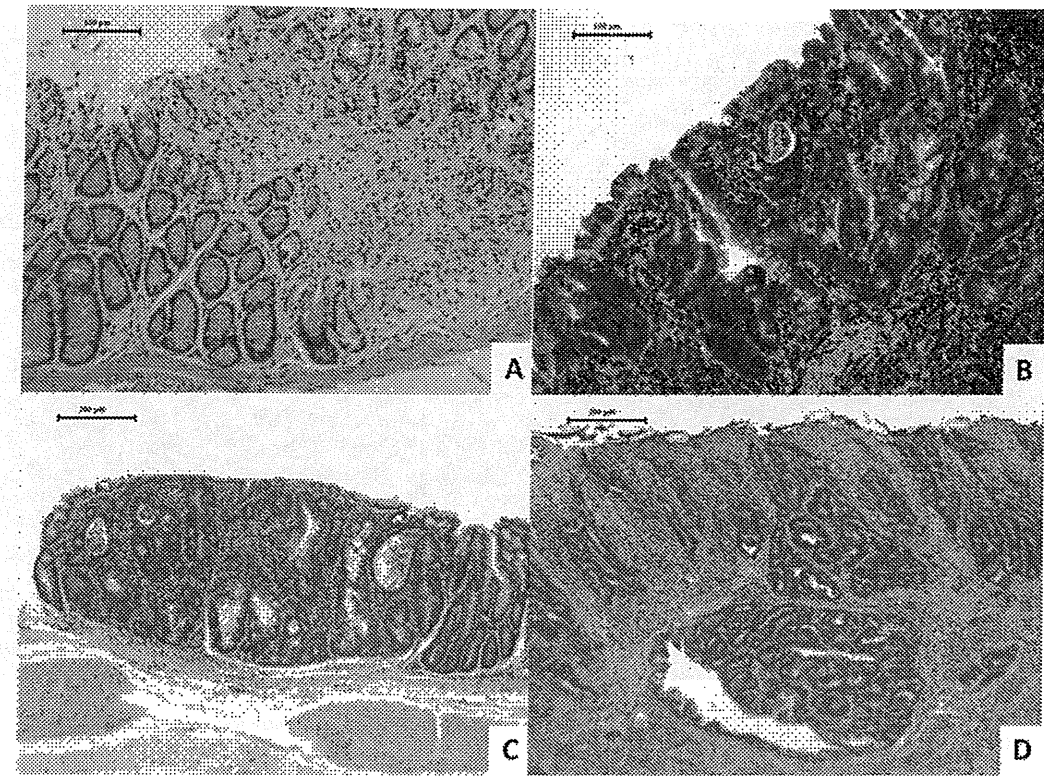

Fig. 2. Representative histopathology of the colonic lesions in mice of group 1 (AOM/DSS). (A) Mucosal ulcer, (B) high-grade dysplastic crypts, (C) tubular adenoma and (D) moderately differentiated tubular adenocarcinoma invaded into submucosa. Bars are 100 μm (A and B) and 200 μm (C and D).

The effects of organo-Mg on the MI and ABI

The exposure to organo-Mg affected the number of mitosis (Figure 5A) and anaphase bridging (Figure 5B) in adenocarcinomas. As illustrated in Figure 5A, drinking with organo-Mg significantly decreased the MI in groups 3 (21.1 ± 7.3, $P < 0.01$) and 4 (19.2 ± 4.4, $P < 0.01$) compared with group 1 (27.0 ± 7.2). The treatment also lowered the ABI in group 3 (2.41 ± 0.91, $P < 0.05$) and group 4 (1.67 ± 0.78, $P < 0.01$) compared with group 1 (3.57 ± 2.06) as shown in Figure 5B.

Expressions of inflammatory enzyme and cytokine genes in colonic mucosa

At week 4, we assayed mRNA levels of TNF-α, IL-1β, IL-6, IFN-γ, iNOS, COX-2 and Nrf2 in the non-lesional colonic mucosa of mice in groups 1 through 6 by quantitative real-time RT–PCR. AOM and DSS treatment increased mRNA expression of TNF-α, IL-1β, IL-6, IFN-γ, iNOS and COX-2 and lowered mRNA expression of Nrf2 when compared with the untreated group (Figure 6A–G). When given organo-Mg (35 and 175 p.p.m.) to mice, mRNA expression of IL-1β (Figure 6B, $P < 0.001$ at both doses). IL-6 (Figure 6C, $P < 0.05$ at 35 p.p.m. and $P < 0.01$ at 175 p.p.m.), IFN-γ (Figure 6D, $P < 0.001$ at both doses) and iNOS (Figure 6E, $P < 0.001$ at both doses) were significatly decreased when compared with the AOM and DSS group. Organo-Mg treatment even at the lowest dose of 7 p.p.m. was able to lower significantly IFN-γ ($P < 0.01$) and iNOS ($P < 0.01$) mRNA expression. Alterations in the mRNA expression of TNF-α (Figure 6A) and COX-2 (Figure 6F) by organo-Mg treatment were not significant. As to Nrf2 mRNA expression, organo-Mg treatment at 35 and 175 p.p.m. significantly increased the expression ($P < 0.001$ at both doses, Figure 6G).

Table II. Incidence (%) and multiplicity (no. of lesions/colon) of colonic lesions

Group no.	Treatment (No. of mice at week 16)	Inflammation score	Mucosal ulcer	Dysplastic crypts (high grade)	Adenoma (AD)	Adenocarcinoma (ADC)	Total tumors (AD + ADC)
1	AOM/DSS (16)	2.06 ± 0.93^a	81% 1.69 ± 1.20	100% 3.75 ± 2.14	81% 2.31 ± 1.92	88% 4.00 ± 2.19	94% 6.31 ± 3.20
2	AOM/DSS/7 p.p.m. organo-Mg (15)	1.20 ± 0.86^b	67% 1.07 ± 0.96	80% 2.67 ± 1.63	73% 1.20 ± 1.26	73% 2.00 ± 1.93^c	80% 3.20 ± 2.68^c
3	AOM/DSS/35 p.p.m. organo-Mg (16)	0.88 ± 0.89^c	44%[d] 0.69 ± 0.87^b	81% 2.00 ± 1.59^b	56% 1.06 ± 1.29	81% 1.81 ± 1.42^e	81% 2.88 ± 2.31^e
4	AOM/DSS/175 ppm organo-Mg (15)	0.60 ± 0.63^c	47% 0.53 ± 0.64^e	80% 1.53 ± 1.46^e	27%[f] 0.47 ± 0.92^e	47%[f] 0.80 ± 1.01^c	47%[f] 1.27 ± 1.71^c
5	175 ppm organo-Mg (6)	0.170.41	0%	0%	0%	0%	0%
6	None (7)	0.120.38	0%	0%	0%	0%	0%

[a]Mean ± SD.
[b]Significantly different from group 1 ([b]$P < 0.05$, [d]$P < 0.01$, and [c]$P < 0.001$) by one-way analysis of variance with Tukey's multiple comparisons test.
[c]Significantly different from group 1 ([b]$P < 0.05$, [e]$P < 0.01$, and [c]$P < 0.001$) by one-way analysis of variance with Tukey's multiple comparisons test.
[d]Significantly different from group 1 ([d]$P < 0.05$ and [f]$P < 0.01$) by Fisher's exact probability test.
[e]Significantly different from group 1 ([d]$P < 0.05$ and [f]$P < 0.01$) by Fisher's exact probability test.
[f]Significantly different from group 1 ([b]$P < 0.05$, [d]$P < 0.01$ and [c]$P < 0.001$) by one-way analysis of variance with Tukey's multiple comparisons test.

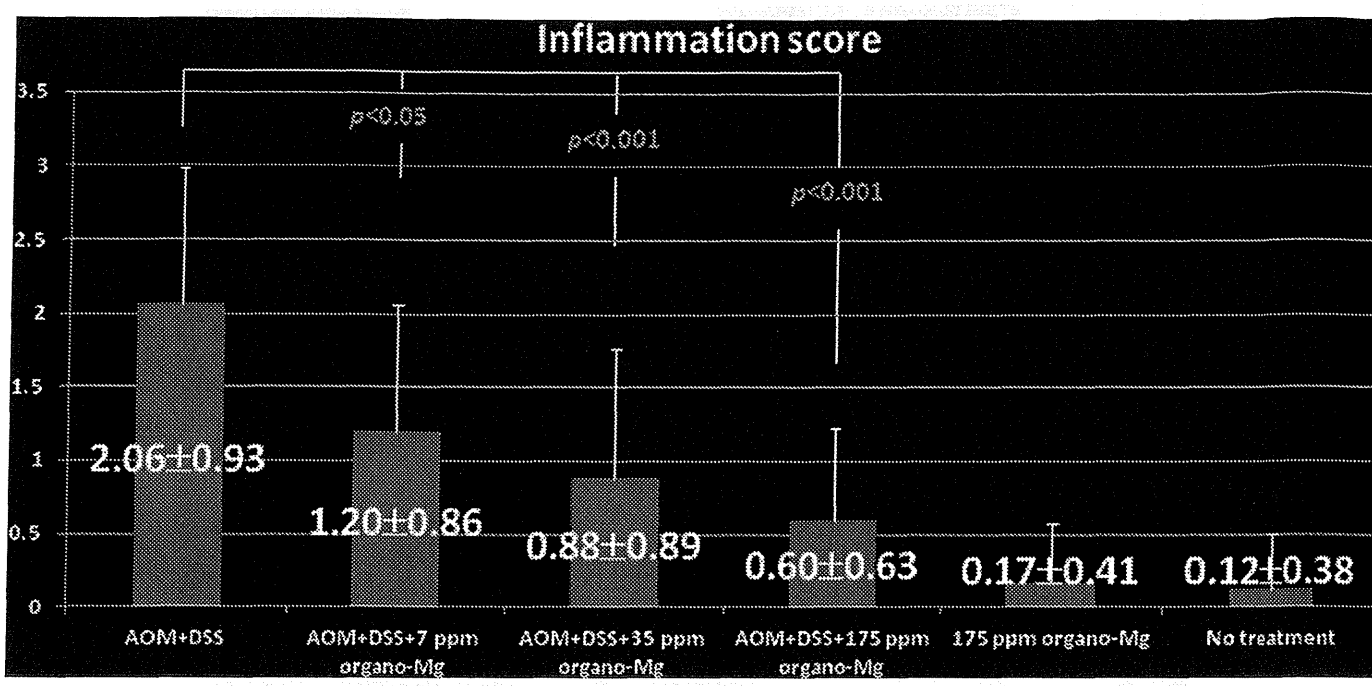

Fig. 3. Inflammation scores of colorectum in all groups. Administration of organo-Mg in drinking water significantly lowered the score of inflammation in the colorectum at 7 p.p.m. ($P < 0.05$), 35 p.p.m. ($P < 0.001$) and 175 p.p.m. ($P < 0.001$).

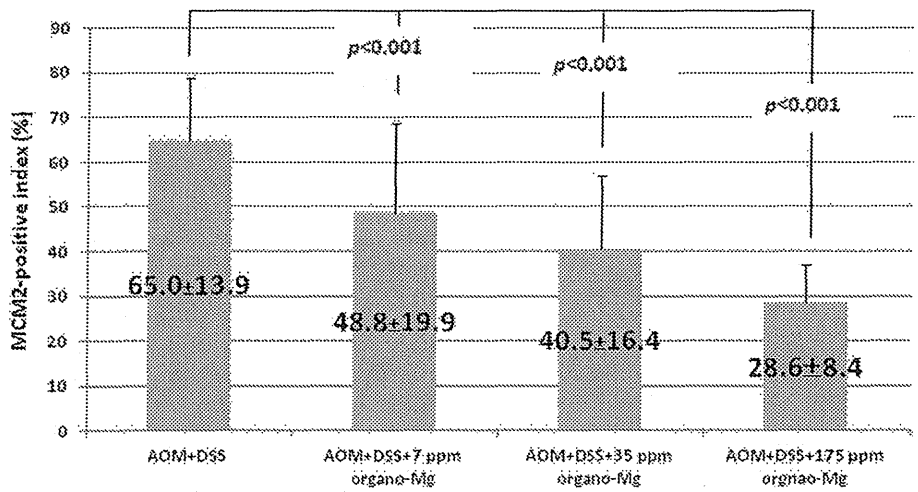

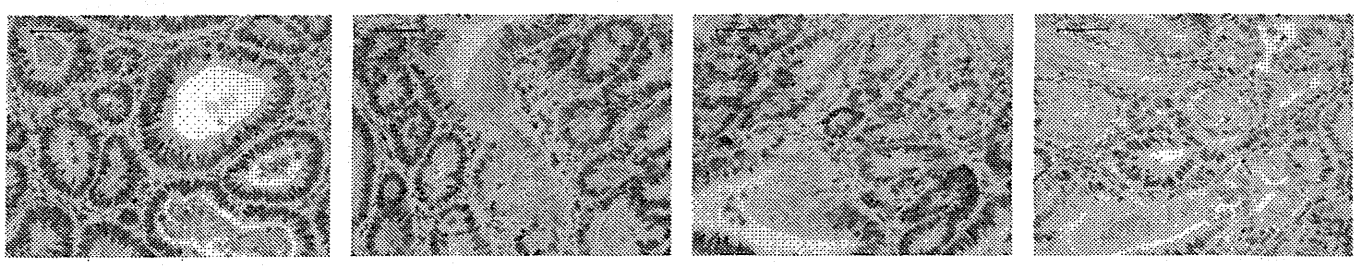

Fig. 4. The MCM2-positive indices (%) of adenocarcinoma cells. Administration with organo-Mg (group 2, $P < 0.001$; group 3, $P < 0.001$; group 4, $P < 0.01$) significantly lowered MCM2-positive indices of adenocarcinoma cells when compared with group 1. The MCM2-positive index (mean ± SD) of normal crypts ($n = 10$) was 6.20 ± 1.99.

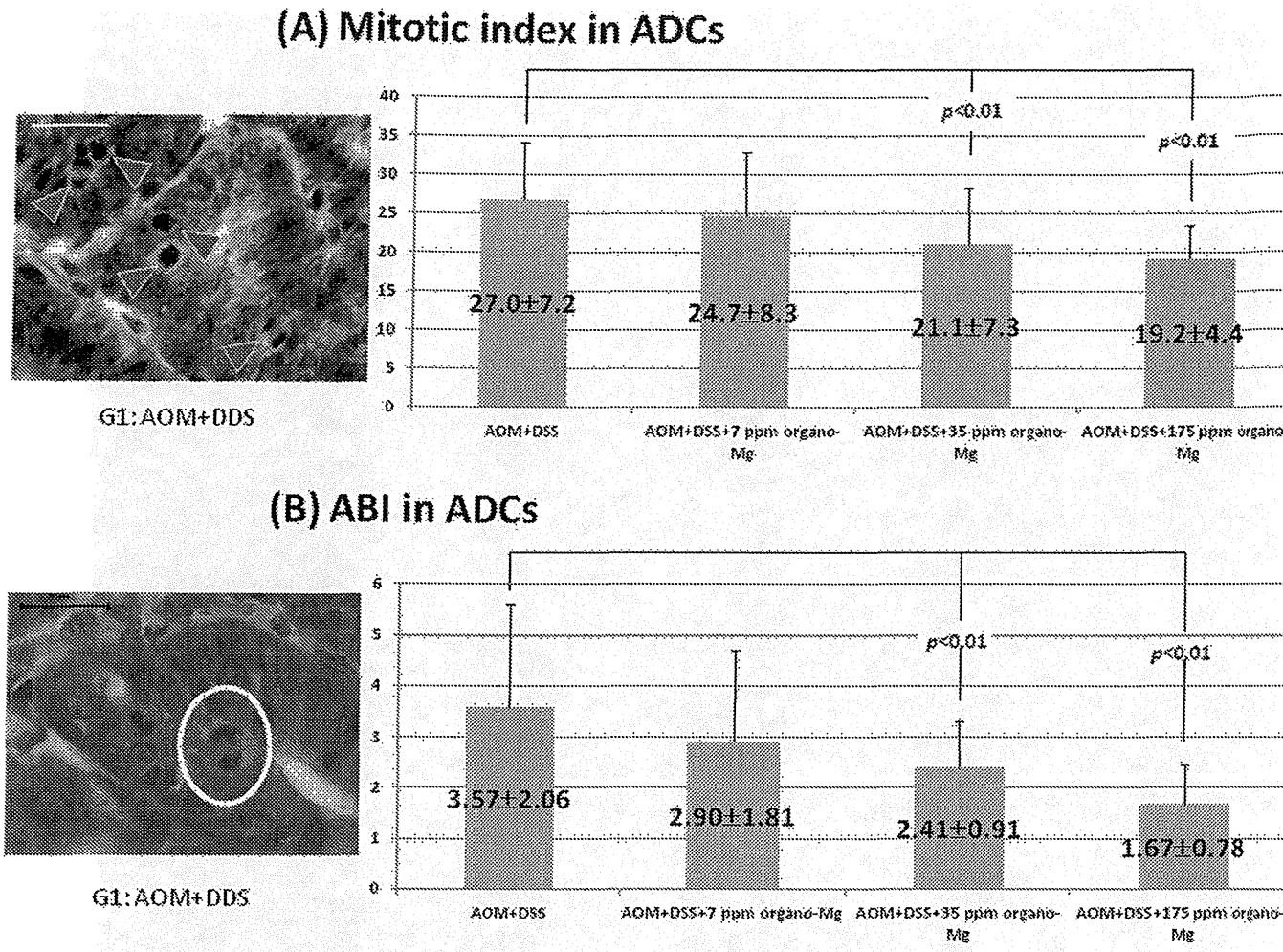

Fig. 5. Effects of organo-Mg on numbers of (A) MI and (B) ABI in adenocarcinomas. Mitotic figures (arrow heads) and anaphase bridging (circled) were observed in adenocarcinomas. Administration with organo-Mg in the drinking water significantly reduced the MI (35 p.p.m., $P < 0.05$; and 175 p.p.m., $P < 0.01$) and ABI (35 p.p.m., $P < 0.05$; 175 p.p.m., $P < 0.01$). The MI (mean ± SD) and ABI (mean ± SD) of normal crypts ($n = 10$) were 3.60±1.26 and 0.10±0.32, respectively.

Antiproliferative effect of organo-Mg on DLD-1 cells

Cell viabilities after organo-Mg/ml medium were as follows in DLD-1 cells: 1 μg, 103.0±2.3%; 10 μg, 102.6±1.0%; 100 μg, 87.6±6.5%; 1000 μg, 84.7±1.2%. The vehicle alone (water) showed no effect on cell proliferation in cancer cells. Adding 1 and 10 μg/ml concentrations of organo-Mg in the medium did not affect the growth of DLD-1 cells. However, 100 and 1000 μg/ml of organo-Mg slightly lowered the growth of DLD-1 cells and the inhibition by 1000 μg/ml organo-Mg was statistically significant ($P < 0.01$) when compared with 0 μg/ml organo-Mg.

Discussion

In this study, we demonstrated that organo-Mg consumption in drinking water at three dose levels (7, 35 and 175 p.p.m.) significantly inhibited AOM/DSS-induced colonrectal carcinogenesis, a model for human colon cancer, in male ICR mice. Even the low dose (7 p.p.m.) of organo-Mg significantly inhibited the development of adenocarcinomas induced by AOM and DSS. The treatment with organo-Mg resulted in reduction of the MCM2-positive index, MI and ABI in the colonic epithelial malignancies at week 16. Organo-Mg in drinking water also affected mRNA expression of certain proinflammatory cytokines (TNF-α, IL1-β and IL-6), inducible inflammatory enzymes (COX-2 and iNOS) and Nrf2 in the colonic mucosa. These effects of organo-Mg may contribute to its suppression effects on AOM/DSS-induced colorectal carcinogenesis in mice. Our results confirmed utility of Mg for prevention of CRC development in humans (8,9) and our earlier experimental study (10).

The effects of organo-Mg on the ABI in the current study are interesting because human UC and UC-associated CRC have high frequency of chromosomal instability (CIN) when compared with colitis other than inflammatory bowel disease and sporadic CRC (15,16). Inflammation in several tissues increases genetic instability, including CIN and microsatellite instability, that contributes to colorectal carcinogenesis, especially colitis-associated CRC development. CIN results in abnormal segregation of chromosomes and abnormal DNA content (aneuploidy). As a result, loss of chromosomal material (loss of heterozygosity) often occur, such as *APC* and *p53*. A high frequency of microsatellite instability and *p53* mutations are detected in UC patients even whose colonic mucosa was negative for dysplasia (28,29). Experimentally, CIN in adenocarcinomas induced by AOM and DSS was quite high (30), whereas the one induced by AOM alone did not show CIN (31). Thus, the AOM/DSS model (19) used in this study is useful for investigating pathogenesis and chemoprevention of colitis-associated colorectal carcinogenesis.

Several epidemiological studies have provided evidence that a correlation exists between dietary Mg and various types of cancer. High levels of Mg in drinking water protect against oesophageal and liver cancer (32,33). Mg concentration in drinking water and/or other dietary sources is inversely correlated with death from

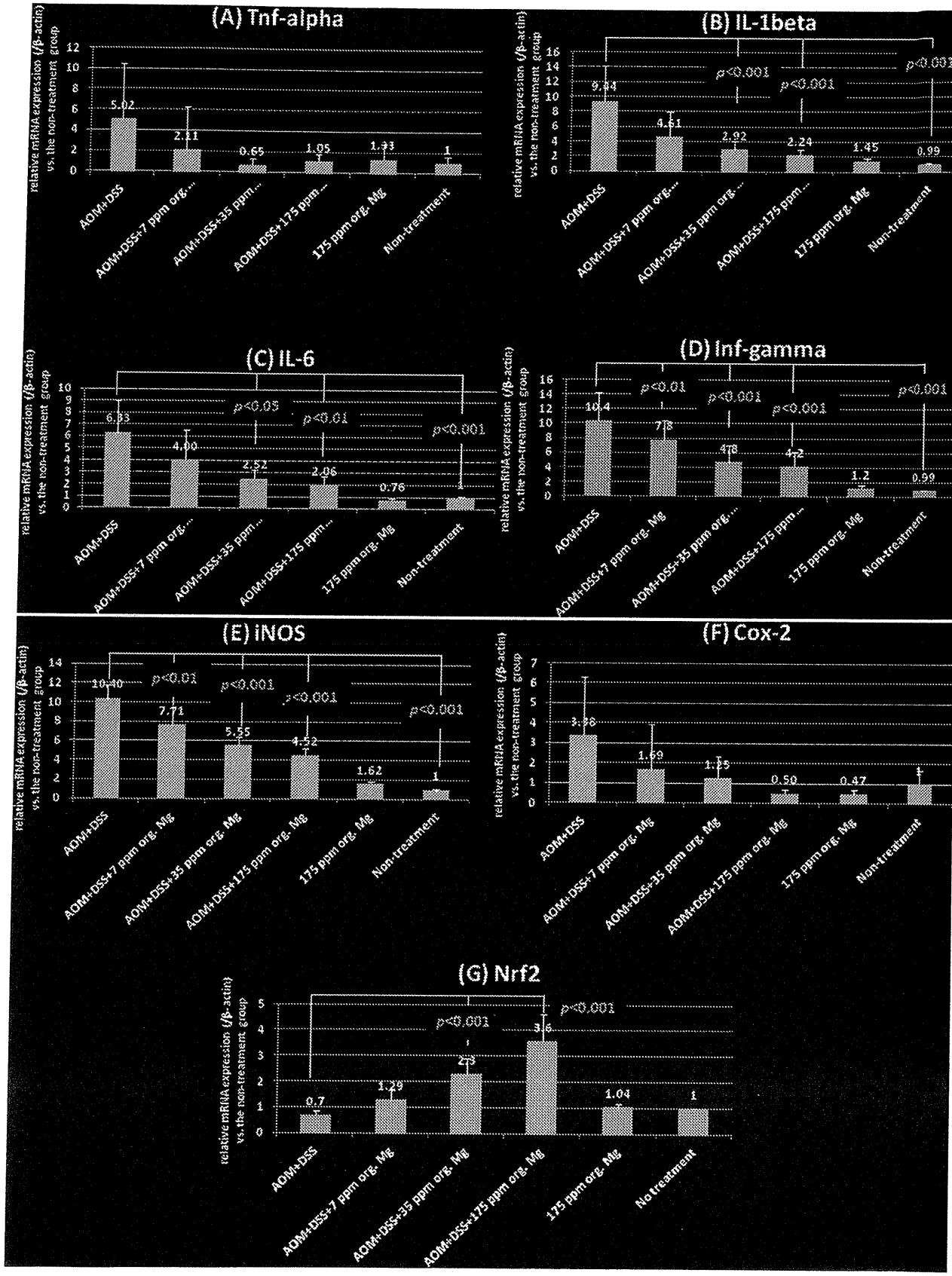

Fig. 6. The mRNA expression levels of (A) TNF-α, (B) IL-1β, (C) IL-6, (D) INF-γ, (E) iNOS, (F) COX-2 and (G) Nrf2 in lesion-free colonic mucosa of all the groups that were assessed by the quantitative real-time RT–PCR. Organo-Mg in the drinking water significantly lowered the expression level of IL-1β (35 and 175 p.p.m.), IL-6 (35 and 175 p.p.m.), iNOS (7, 35 and 175 p.p.m.) and IFN-γ (7, 35 and 175 ppm) when compared with the AOM and DSS group. The expression was normalized to β-actin mRNA expression. Samples were analyzed in triplicate. Data are mean ± SD from three independent assays ($n = 5$ from each group). Statistical analysis was performed by Kruskal–Wallis test. Ordinates are relative mRNA expression (β-actin) versus the non-treatment group.

breast, prostate, ovarian cancers and risk of lung cancer (34–37). An association between low intake of Mg and the risk of colon cancer is indicated by several epidemiological studies conducted in various countries (9,38–40). Furthermore, a significant inverse correlation between dietary intake of Mg and colon cancer in men was revealed by a large population-based prospective study in Japan (8).

Experimental Mg deficiency using rat induces a clinical inflammatory syndrome characterized by leukocyte and macrophage activation, release of inflammatory cytokines and acute phase proteins, excessive production of free radicals (17). A low Mg status has been clearly associated with increased inflammatory stress in humans (41). Inflammation promotes not only in the early stages of tumorigenesis by inducing genetic instability but also in the late events, invasion and metastasis through inflammatory mediators induction (18). In the current study, we observed cancer chemopreventive activity of organo-Mg in carcinogenesis in the inflamed colon of mice. In addition, treatment with organo-Mg in the drinking water lowered the occurrence of mucosal ulcers and preneoplasms, high-grade dysplastic crypts. Interestingly, we observed that organo-Mg in the drinking water lowered the expression of proinflammatory chemokines in the colonic mucosa without tumors. It is reported that the anti-inflammatory action of Mg is caused by its ability to inactivate lipopolysaccharides and to inhibit expression of several proinflammatory cytokines such as TNF-α, IL-6 and NF-κB in human placental cell, monocyte and murine macrophage-like RAW264.7 cells (42–44). In Mg-deficient mice, higher expressions of TNF-α and IL-6 have not always been observed in colonic mucosa (45). This may be caused by alterations in intestinal bifidobacteria levels. Further studies are needed to assess the role of Mg in intestinal microflora in colitis-associated colorectal carcinogenesis model that was used in this study (46).

Other interesting findings regarding mRNA expression of several proteins are that organo-Mg could increase Nrf2 mRNA expression. Increased susceptibility to colitis-related CRC (21) and aberrant crypt foci (23) was reported in Nrf2-deficient mice. On the other hand, activation of Nrf2 signaling resulted in suppression of colitis-associated CRC (22,47–49). It may be possible that increased mRNA expression of Nrf2 by organo-Mg treatment in the inflamed colonic mucosa contributes suppressive effects of organo-Mg on inflammation-associated colorectal carcinogenesis. Additional studies are planed in our laboratory to confirm our results on mRNA expression of Nrf2 in different experimental models of colorectal carcinogenesis with and without inflammatory stimuli.

We can point other mechanisms by which organo-Mg may suppress AOM/DSS-induced colon carcinogenesis in this study. Organo-Mg lowered MCM2-positive index and MI of colonic adenocarcinomas may suggest antigrowth effects of organo-Mg on colonic malignancy. Binding of Mg ions to DNA reduces locally the negative charge density and changes the protection pattern of DNA from hydroxyl radicals (50). Mg is highly required to maintain genomic stability and to remove of DNA damage generated by environmental mutagens, endogenous processes and for DNA replication as an essential cofactor for several enzyme systems involving DNA repair such as nucleotide excision repair, base excision repair and mismatch repair (51). Our data on the effects of organo-Mg on the ABI of adenocarcinoma cells may suggest that organo-Mg is able to affect the CIN of cancer cells (52). In our *in vitro* experiment in this study, addition of a high dose (1000 μg/ml) of organo-Mg to the culture medium resulted in slight inhibition of the growth of human colorectal adenocarcinoma cell line, DLD-1 (15% inhibition, $P < 0.01$). However, the dose (1000 μg/ml) was quite high, suggesting cytotoxic effects of organo-Mg. We therefore should evaluate potential antigrowth effects of organo-Mg on another human colorectal cancer cell lines.

In conclusion, organo-Mg in the drinking water effectively suppressed AOM/DSS-induced mouse colon carcinogenesis by lowering proliferation and CIN in colonic adenocarcinomas in conjunction with by suppressing mRNA expression of several proinflammatory cytokines (IL-1β, IL-6, IFN-γ) and an inducible inflammatory enzyme (iNOS) and activating Nrf2 mRNA expression. Additional in-depth studies on the effects of organo-Mg on the intestinal microflora in the colitis-associated colorectal carcinogenesis model are needed to gain further understanding of the mode of action of organo-Mg in inflammation-related carcinogenesis and to develop novel approaches for prevention of CRC in inflamed colon.

Funding

Grant-in-Aid for the 2nd and 3rd Terms Comprehensive 10-Year Strategy for Cancer Control from the Ministry of Health and Welfare of Japan and Grants-in-Aid (13671986 and 23501324) from the Ministry of Education, Science, Sports and Culture of Japan.

Acknowledgements

Organo-Mg was kindly supplied by Tateho Chemical Industries Co., Ltd. (COE: Testunori Minato, Ako City, Hyogo, Japan) and Air Water Inc. (COE: Hiroshi Aoki, Sapporo, Japan).

Conflict of Interest Statement: None declared.

References

1. Karim-Kos,H.E. *et al.* (2008) Recent trends of cancer in Europe: a combined approach of incidence, survival and mortality for 17 cancer sites since the 1990s. *Eur. J. Cancer*, **44**, 1345–1389.
2. Siegel,R. *et al.* (2011) Cancer statistics, 2011: the impact of eliminating socioeconomic and racial disparities on premature cancer deaths. *CA. Cancer J. Clin.*, **61**, 212–236.
3. Tenesa,A. *et al.* (2009) New insights into the aetiology of colorectal cancer from genome-wide association studies. *Nat. Rev. Genet.*, **10**, 353–358.
4. Barbagallo,M. *et al.* (2003) Role of magnesium in insulin action, diabetes and cardio-metabolic syndrome X. *Mol. Aspects Med.*, **24**, 39–52.
5. Houston,M. (2011) The role of magnesium in hypertension and cardiovascular disease. *J. Clin. Hypertens. (Greenwich).*, **13**, 843–847.
6. Belin,R.J. *et al.* (2007) Magnesium physiology and pathogenic mechanisms that contribute to the development of the metabolic syndrome. *Magnes. Res.*, **20**, 107–129.
7. Rosanoff,A. *et al.* (2012) Suboptimal magnesium status in the United States: are the health consequences underestimated? *Nutr. Rev.*, **70**, 153–164.
8. Ma,E. *et al.* (2010) High dietary intake of magnesium may decrease risk of colorectal cancer in Japanese men. *J. Nutr.*, **140**, 779–785.
9. van den Brandt,P.A. *et al.* (2007) Magnesium intake and colorectal cancer risk in the Netherlands Cohort Study. *Br. J. Cancer*, **96**, 510–513.
10. Tanaka,T. *et al.* (1989) Inhibitory effect of magnesium hydroxide on methylazoxymethanol acetate-induced large bowel carcinogenesis in male F344 rats. *Carcinogenesis*, **10**, 613–616.
11. Wang,A. *et al.* (1993) Inhibitory effects of magnesium hydroxide on c-myc expression and cell proliferation induced by methylazoxymethanol acetate in rat colon. *Cancer Lett.*, **75**, 73–78.
12. Tanaka,T. (2009) Colorectal carcinogenesis: Review of human and experimental animal studies. *J. Carcinog.*, **8**, 5.
13. Befrits,R. *et al.* (1994) DNA aneuploidy and histologic dysplasia in long-standing ulcerative colitis. A 10-year follow-up study. *Dis. Colon Rectum*, **37**, 313–9; discussion 319.
14. Habermann,J. *et al.* (2001) Ulcerative colitis and colorectal carcinoma: DNA-profile, laminin-5 gamma2 chain and cyclin A expression as early markers for risk assessment. *Scand. J. Gastroenterol.*, **36**, 751–758.
15. Araujo,S.E. *et al.* (2007) DNA ploidy status and prognosis in colorectal cancer: a meta-analysis of published data. *Dis. Colon Rectum*, **50**, 1800–1810.
16. Gerling,M. *et al.* (2010) High Frequency of Aneuploidy Defines Ulcerative Colitis-Associated Carcinomas: A Comparative Prognostic Study to Sporadic Colorectal Carcinomas. *Ann. Surg.*, **252**, 84–89.
17. Mazur,A. *et al.* (2007) Magnesium and the inflammatory response: potential physiopathological implications. *Arch. Biochem. Biophys.*, **458**, 48–56.
18. Colotta,F. *et al.* (2009) Cancer-related inflammation, the seventh hallmark of cancer: links to genetic instability. *Carcinogenesis*, **30**, 1073–1081.

19. Tanaka,T. *et al.* (2003) A novel inflammation-related mouse colon carcinogenesis model induced by azoxymethane and dextran sodium sulfate. *Cancer Sci.*, **94**, 965–973.
20. Tanaka,T. *et al.* (2001) Ligands for peroxisome proliferator-activated receptors alpha and gamma inhibit chemically induced colitis and formation of aberrant crypt foci in rats. *Cancer Res.*, **61**, 2424–2428.
21. Khor,T.O. *et al.* (2008) Increased susceptibility of Nrf2 knockout mice to colitis-associated colorectal cancer. *Cancer Prev. Res. (Phila).*, **1**, 187–191.
22. Li,W. *et al.* (2008) Activation of Nrf2-antioxidant signaling attenuates NFkappaB-inflammatory response and elicits apoptosis. *Biochem. Pharmacol.*, **76**, 1485–1489.
23. Osburn,W.O. *et al.* (2007) Increased colonic inflammatory injury and formation of aberrant crypt foci in Nrf2-deficient mice upon dextran sulfate treatment. *Int. J. Cancer*, **121**, 1883–1891.
24. Rudolph,K.L. *et al.* (2001) Telomere dysfunction and evolution of intestinal carcinoma in mice and humans. *Nat. Genet.*, **28**, 155–159.
25. Oyama,T. *et al.* (2009) Dietary tricin suppresses inflammation-related colon carcinogenesis in male Crj: CD-1 mice. *Cancer Prev. Res. (Phila).*, **2**, 1031–1038.
26. Suzuki,R. *et al.* (2005) Dose-dependent promoting effect of dextran sodium sulfate on mouse colon carcinogenesis initiated with azoxymethane. *Histol. Histopathol.*, **20**, 483–492.
27. Hanna-Morris,A. *et al.* (2009) Minichromosome maintenance protein 2 (MCM2) is a stronger discriminator of increased proliferation in mucosa adjacent to colorectal cancer than Ki-67. *J. Clin. Pathol.*, **62**, 325–330.
28. Brentnall,T.A. *et al.* (1996) Microsatellite instability in nonneoplastic mucosa from patients with chronic ulcerative colitis. *Cancer Res.*, **56**, 1237–1240.
29. Hussain,S.P. *et al.* (2000) Increased p53 mutation load in noncancerous colon tissue from ulcerative colitis: a cancer-prone chronic inflammatory disease. *Cancer Res.*, **60**, 3333–3337.
30. Gerling,M. *et al.* (2011) Characterization of chromosomal instability in murine colitis-associated colorectal cancer. *PLoS ONE*, **6**, e22114.
31. Guda,K. *et al.* (2004) Carcinogen-induced colon tumors in mice are chromosomally stable and are characterized by low-level microsatellite instability. *Oncogene*, **23**, 3813–3821.
32. Tukiendorf,A. *et al.* (2004) New data on ecological analysis of possible relationship between magnesium in drinking water and liver cancer. *Magnes. Res.*, **17**, 46–52.
33. Yang,C.Y. *et al.* (2002) Magnesium and calcium in drinking water and the risk of death from esophageal cancer. *Magnes. Res.*, **15**, 215–222.
34. Chiu,H.F. *et al.* (2004) Magnesium and calcium in drinking water and risk of death from ovarian cancer. *Magnes. Res.*, **17**, 28–34.
35. Mahabir,S. *et al.* (2008) Dietary magnesium and DNA repair capacity as risk factors for lung cancer. *Carcinogenesis*, **29**, 949–956.
36. Yang,C.Y. *et al.* (2000) Calcium and magnesium in drinking water and the risk of death from breast cancer. *J. Toxicol. Environ. Health Part A*, **60**, 231–241.
37. Yang,C.Y. *et al.* (2000) Calcium and magnesium in drinking water and risk of death from prostate cancer. *J. Toxicol. Environ. Health Part A*, **60**, 17–26.
38. Chiu,H.F. *et al.* (2010) Colon cancer and content of nitrates and magnesium in drinking water. *Magnes. Res.*, **23**, 81–89.
39. Folsom,A.R. *et al.* (2006) Magnesium intake and reduced risk of colon cancer in a prospective study of women. *Am. J. Epidemiol.*, **163**, 232–235.
40. Larsson,S.C. *et al.* (2005) Magnesium intake in relation to risk of colorectal cancer in women. *JAMA*, **293**, 86–89.
41. Nielsen,F.H. (2010) Magnesium, inflammation, and obesity in chronic disease. *Nutr. Rev.*, **68**, 333–340.
42. Dowling,O. *et al.* (2012) Magnesium sulfate reduces bacterial LPS-induced inflammation at the maternal-fetal interface. *Placenta*, **33**, 392–398.
43. Liu,Z. *et al.* (2012) Magnesium sulfate inhibits the secretion of high mobility group box 1 from lipopolysaccharide-activated RAW264.7 macrophages in vitro. *J. Surg. Res.*, in press.
44. Sugimoto,J. *et al.* (2012) Magnesium decreases inflammatory cytokine production: a novel innate immunomodulatory mechanism. *J. Immunol.*, **188**, 6338–6346.
45. Pachikian,B.D. *et al.* (2010) Changes in intestinal bifidobacteria levels are associated with the inflammatory response in magnesium-deficient mice. *J. Nutr.*, **140**, 509–514.
46. Uronis,J.M. *et al.* (2009) Modulation of the intestinal microbiota alters colitis-associated colorectal cancer susceptibility. *PLoS ONE*, **4**, e6026.
47. Chiou,Y.S. *et al.* (2012) Peracetylated (-)-epigallocatechin-3-gallate (AcEGCG) potently suppresses dextran sulfate sodium-induced colitis and colon tumorigenesis in mice. *J. Agric. Food Chem.*, **60**, 3441–3451.
48. Krehl,S. *et al.* (2012) Glutathione peroxidase-2 and selenium decreased inflammation and tumors in a mouse model of inflammation-associated carcinogenesis whereas sulforaphane effects differed with selenium supply. *Carcinogenesis*, **33**, 620–628.
49. Theiss,A.L. *et al.* (2009) Prohibitin is a novel regulator of antioxidant response that attenuates colonic inflammation in mice. *Gastroenterology*, **137**, 199–208, 208.e1.
50. Anastassopoulou,J. *et al.* (2002) Magnesium-DNA interactions and the possible relation of magnesium to carcinogenesis. Irradiation and free radicals. *Crit. Rev. Oncol. Hematol.*, **42**, 79–91.
51. Hartwig,A. (2001) Role of magnesium in genomic stability. *Mutat. Res.*, **475**, 113–121.
52. Stewénius,Y. *et al.* (2005) Structural and numerical chromosome changes in colon cancer develop through telomere-mediated anaphase bridges, not through mitotic multipolarity. *Proc. Natl. Acad. Sci. U.S.A.*, **102**, 5541–5546.

Received July 30, 2012; revised October 19, 2012; accepted October 23, 2012

Published OnlineFirst February 2, 2010; DOI: 10.1158/0008-5472.CAN-09-2755

AACR

Cancer Research

Inflammatory Processes Triggered by *Helicobacter pylori* Infection Cause Aberrant DNA Methylation in Gastric Epithelial Cells

Tohru Niwa, Tetsuya Tsukamoto, Takeshi Toyoda, et al.

Cancer Res 2010;70:1430-1440. Published OnlineFirst February 2, 2010.

Published OnlineFirst February 2, 2010; DOI: 10.1158/0008-5472.CAN-09-2755

Molecular and Cellular Pathobiology

Cancer Research

Inflammatory Processes Triggered by *Helicobacter pylori* Infection Cause Aberrant DNA Methylation in Gastric Epithelial Cells

Tohru Niwa[1], Tetsuya Tsukamoto[2], Takeshi Toyoda[2], Akiko Mori[1], Harunari Tanaka[2], Takao Maekita[3], Masao Ichinose[3], Masae Tatematsu[2], and Toshikazu Ushijima[1]

Abstract

Altered patterns of DNA methylation associated with *Helicobacter pylori* (*HP*) infection of gastric epithelial cells are thought to contribute to gastric cancer risk. However, it is unclear whether this increased risk reflects an infection-associated inflammatory response or the infection itself. In this study, we sought to clarify mechanisms in a gerbil model of gastric cancer where we showed that *HP* infection is causally involved in induction of aberrant DNA methylation. By genome-wide screening, CpG islands that were aberrantly methylated in gerbil gastric cancer cell lines were isolated, and 10 islands were shown to be specifically methylated only in gastric mucosae infected with *HP*. By temporal analysis, methylation levels in gastric epithelial cells started to increase at 5 to 10 weeks after infection and reached high levels by 50 weeks. When *HP* was eradicated, methylation levels markedly decreased 10 and 20 weeks later, but they remained higher than those in gerbils that were not infected by *HP*. Expression levels of several inflammation-related genes (*CXCL2, IL-1β, NOS2*, and *TNF-α*) paralleled the temporal changes of methylation levels. Significantly suppressing inflammation with the immunosuppressive drug cyclosporin A did not affect colonization by *HP* but blocked the induction of altered DNA methylation. Our findings argue that DNA methylation alterations that occur in gastric mucosae after *HP* infection are composed of transient components and permanent components, and that it is the infection-associated inflammatory response, rather than *HP* itself, which is responsible for inducing the altered DNA methylation. *Cancer Res; 70(4); 1430–40. ©2010 AACR.*

Introduction

Aberrant DNA methylation of promoter CpG islands (CGI) is one of the major inactivating mechanisms of tumor-suppressor genes and is deeply involved in human carcinogenesis (1). Nevertheless, there is only limited information on its inducers and induction mechanisms. Chronic inflammation, known to promote certain types of cancers (2), is one of the possible inducers of aberrant methylation. The presence of aberrant methylation is frequently observed in noncancerous tissues of patients with inflammation-associated cancers, such as liver cancers, ulcerative colitis–associated colon cancers, and gastric cancers (3–7). However, a causal role of chronic inflammation in methylation induction remains to be established.

Authors' Affiliations: [1]Carcinogenesis Division, National Cancer Center Research Institute, Chuo-ku, Tokyo, Japan; [2]Division of Oncological Pathology, Aichi Cancer Center Research Institute, Chikusa, Nagoya, Japan; and [3]Second Department of Internal Medicine, Wakayama Medical University, Wakayama, Japan

Note: Supplementary data for this article are available at Cancer Research Online (http://cancerres.aacrjournals.org/).

Corresponding Author: Toshikazu Ushijima, Carcinogenesis Division, National Cancer Center Research Institute, 5-1-1-Tsukiji, Chuo-ku, Tokyo 104-0045, Japan. Phone: 81-3-3542-2511; Fax: 81-3-5565-1753; E-mail: tushijim@ncc.go.jp.

doi: 10.1158/0008-5472.CAN-09-2755

In human gastric mucosae, the presence of *Helicobacter pylori* (*HP*) infection, a well-known inducer of chronic inflammation and gastric cancers (8, 9), is associated with high methylation levels or high incidences of methylation (5, 10–12). In addition, among individuals without *HP* infection, noncancerous gastric mucosae of gastric cancer patients have higher methylation levels than gastric mucosae of healthy individuals (5, 10). In addition, eradication of *HP* leads to a decreased incidence of *CDH1* (*E-cadherin*) promoter methylation (11, 13, 14). These findings suggest that *HP* infection induces aberrant methylation in gastric mucosae and indicate that levels of accumulated methylation are associated with gastric cancer risk. However, because infection experiments are impossible in humans, it needs to be clarified in animal models whether or not *HP* infection induces methylation and what mechanisms are involved.

HP infection in humans is best modeled in Mongolian gerbils (*Meriones unguiculatus*). As in man, *HP* infection induces severe inflammation in gerbil gastric mucosae and promotes gastric carcinogenesis induced by administration of *N*-methyl-*N*-nitrosourea (MNU) or *N*-methyl-*N'*-nitrosoguanidine (15). The incidence of gastric cancers in gerbils depends on the duration of *HP* infection, and eradication of *HP* significantly reduces the incidence (16), as in man (17, 18). Thus, we can expect that the gerbil model is also useful in analyzing whether *HP* infection induces aberrant methylation and what mechanisms are involved *in vivo*. However, unfortunately,

Published OnlineFirst February 2, 2010; DOI: 10.1158/0008-5472.CAN-09-2755

little information is available for the gerbil genome, and the genetic and molecular analysis of this model has been hampered.

In this study, we aimed to show that *HP* infection is causally involved in induction of aberrant DNA methylation and to clarify a critical factor involved. For this, we first isolated CGIs that could be methylated in gerbil gastric cancers by a genome-wide screening method, methylation-sensitive representational difference analysis (MS-RDA). Using the CGIs isolated, we then showed that methylation was induced specifically in gerbils with *HP* infection and that inflammation induced by *HP* infection, not *HP* itself, was critically involved in methylation induction.

Materials and Methods

Cell lines. Two gerbil gastric cancer cell lines, MGC1 and MGC2, were established from a single gastric cancer induced in a gerbil by MNU and *HP* infection (19). They were maintained in RPMI 1640 supplemented with 10% fetal bovine serum on a type I collagen–coated dish (Asahi Techno Glass). Although we did not check the cross-contamination of cell lines biochemically or genetically just before use, they had the same morphology and growth rates as described previously (19).

Animal experiments and sample preparation. Male Mongolian gerbils (MGS/Sea) were purchased from Kyudo. To induce gastric cancers, male gerbils were administrated with 30 ppm of MNU (Sigma-Aldrich) in drinking water for a week at 7, 9, 11, 13, and 15 wk of age, and then inoculated with *HP* (ATCC 43504, American Type Culture Collection) by gavage at 17 wk of age (20). At 57 wk, gerbils were sacrificed and stomachs were resected. Because it was difficult to identify cancers macroscopically in gastric mucosae with severe hyperplasia, we dissected an area of gastric cancer tissue by an apparatus for laser microdissection (ASLMD, Leica Microsystems) after histologic confirmation. For temporal analysis of methylation levels, male gerbils were inoculated with *HP* (ATCC 43504) at 5 wk of age. Eradication therapy was done at 55 wk of age by administering amoxicillin, clarithromycin, and lansoprazole by gavage (20). Gerbils that had *HP* after the eradication therapy were excluded from analysis. As a vehicle control, 0.5% of carboxymethyl cellulose was given by gavage. To suppress gastritis, gerbils were administered with 250 μg/mL cyclosporin A (CsA; Neoral, Novartis Pharma) in drinking water for 20 wk. The stomach was resected and cut along the greater curvature. From the posterior wall of the pyloric region (pyloric antrum), which contains the pyloric glands, gastric epithelial cells (GEC) were isolated by the gland isolation technique (21). The anterior wall of the pyloric region was further cut into two pieces: one for RNA and DNA extraction from a sample with mucus and mucosal and submucosal layers and the other for histologic analysis. Whole blood was obtained from the inferior vena cava. The animal experiment protocols were approved by the Committee for Ethics in Animal Experimentation.

Human clinical samples. Human gastric mucosae were obtained by endoscopic biopsy from 10 *HP*-negative (five men and five women; average age 42.4 y, ranging from 29 to 56 y) and 10 *HP*-positive (four men and six women; average age 42.4 y, ranging from 23 to 53 y) healthy volunteers, whose *HP* status had been judged by a serum anti-*HP* antibody test (SBS). Gastric cancer samples were obtained from surgical specimens from 14 patients who underwent gastrectomy due to early gastric cancers (seven men and seven women; average age 65.9 y, ranging from 47 to 79 y). Sampling was conducted under the approval of Institutional Review Boards.

Nucleic acid extraction. From tissue sections, DNA was extracted by heating the dissected sections at 100°C for 20 min at pH 12, followed by phenol/chloroform extraction (22). From isolated glands, DNA was extracted by proteinase K digestion and the phenol/chloroform method. From the whole blood, DNA was extracted with a QuickGene DNA whole blood kit (Fujifilm). RNA was isolated with Isogen (Wako).

Quantitative PCR for gene expression analyses and* HP *detection. To analyze gene expression levels, cDNA was synthesized from 2 μg of DNase-treated RNA with an oligo-d $(T)_{12-18}$ primer. Real-time PCR using gene-specific primers (Supplementary Table S1) and SYBR Green Real-time PCR Master Mix (TOYOBO) was done, and the amplification curve of a sample was compared with curves of standard DNA samples with known copy numbers. Standard DNA samples were prepared by serial dilution of a PCR product or a plasmid containing a cloned PCR fragment after its quantification. Gene expression levels were normalized to that of *Gapdh*. To measure the amount of *HP*, real-time PCR using specific primers for the *jhpr3* gene of *HP* was carried out and normalized to the gerbil *Il4* gene (Supplementary Table S1).

Methylation-sensitive representational difference analysis. MS-RDA is a subtraction method that can identify differentially methylated loci between two genomes independent of genomic information (23) and was done using *Hpa*II or *Sac*II methylation-sensitive restriction enzyme as described previously (24). The final PCR product was cloned into pGEM T-Easy (Promega) and sequenced. If a DNA fragment had a CpG score ≥0.65 and G + C content ≥55%, the fragment was considered to be derived from a CGI. To identify homologous regions in mice and men, database searches were carried out at a GenBank web site.

Methylation analysis. Fully methylated and fully unmethylated controls were prepared by methylating genomic DNA with *Sss*I methylase (New England Biolabs) and amplifying genomic DNA with ϕ29 DNA polymerase (GenomiPhi DNA Amplification Kit, GE Healthcare), respectively (25). One microgram of DNA digested with *Bam*HI was treated with sodium bisulfite and suspended in 80 μL of Tris-EDTA (TE) buffer as described previously (22). In the case of paraffin-embedded samples, DNA was treated with sodium bisulfite without *Bam*HI digestion and suspended in 20 μL of TE buffer. One microliter of aliquot was used as a template for methylation-specific PCR (MSP) and bisulfite sequencing. Conventional MSP and bisulfite sequencing were done with specific primer sets (Supplementary Table S2) as described previously (22). Quantitative MSP (qMSP) was done

Published OnlineFirst February 2, 2010; DOI: 10.1158/0008-5472.CAN-09-2755

Table 1. CGIs methylated in gerbil gastric cancer cell lines and *HP*-infected GECs

Clone name	GenBank accession no.	Genomic location deduced from analyses using human or mouse genome database	Nucleotide position in human or mouse sequences
HE6	AB429514	Exon 2 of *Ntrk2* gene*	16,449,514–16,449,840 bp in NT_023935.17 (human chr. 9)
HG2	AB429515	Exon 1 of *Gpr37* gene*	49,589,571–49,589,704 bp in NT_007933.14 (human chr. 7)
SA9	AB429516	Exon 1 of *Nol4* gene*	13,292,105–13,292,430 bp in NT_010966.13 (human chr. 18)
SB1	AB429517	Intergenic region between *Sp4* and *Sp8* genes*	20,698,454–20,698,697 bp in NT_007819.16 (human chr. 7)
SB5	AB429513	Not identified	Not identified
SC3	AB429518	Promoter region of *Rnf152* gene*	7,352,575–7,352,875 bp in NT_025028.13 (human chr. 18)
SD2	AB429519	Promoter region of *Nptx2* gene*	23,480,374–23,480,422 bp in NT_007933.14 (human chr. 7)
SE3	AB429520	Intron 1 of *Slc35f1* gene*	39,311,942–39,312,270 bp in NT_001838990.2 (human chr. 6)
SF12	AB429521	Intergenic region between *Cntn1* and *Pdzm4* genes	53,513,634–53,513,936 bp in NT_039621.7 (mouse chr. 15)
SH6	AB429522	Intergenic region between *Sox1* and *Loc729095* gene*	213,253–213,298 bp in NT_027140.6 (human chr. 13)

*Conserved regions identified in the human database.

by real-time PCR using primers specific to DNA molecules methylated at a locus and to a repeat sequence. Methylation levels were expressed as a percentage of the methylated reference, which was obtained as [(number of methylated fragments of a target CGI in sample) / (number of repeat sequences in sample)] / [(number of methylated fragments of a target CGI in *SssI*-treated DNA) / (number of repeat sequences in *SssI*-treated DNA)] × 100. As a repeat sequence, the B2 repeat was used for gerbil DNA (ref. 26; Supplementary Table S2 and Supplementary Fig. S1) and the *Alu* repeat was used for human DNA (27).

Statistical analysis. Statistical analyses were conducted with SPSS 13.0J (SPSS Japan, Inc.). To evaluate significant difference between two independent groups of sample data, the Mann-Whitney *U* test was used. Spearman's rank correlation coefficient (*r*) was used to measure correlation.

Results

Identification of CGIs specifically methylated by HP infection in GECs of Mongolian gerbils. To identify CGIs methylated in GECs of gerbils with *HP* infection, we adopted the strategy of a genome-wide screening in cancers and high-sensitivity analysis in GECs. The genome-wide screening was done by MS-RDA using a pool of two gerbil gastric cancer cell lines (MGC1 and MGC2) as the driver and GECs of noninfected gerbils as the tester. The final products of two series of MS-RDA using *Hpa*II and *Sac*II were cloned and 180 DNA fragments were sequenced. One hundred three of them were nonredundant, and 56 of them contained a sequence likely to have originated from a CGI. Due to the lack of information on the gerbil genome, we first analyzed the methylation statuses of CpG sites within the DNA fragments isolated using MSP. MSP primers were successfully designed for 27 of the 56 DNA fragments, and we analyzed the two gastric cancer cell lines, five samples of GECs from gerbils infected with *HP* for 50 weeks, and five samples of GECs from age-matched gerbils without infection. Ten (HE6, HG2, SA9, SB1, SB5, SC3, SD2, SE3, SF12, and SH6) of the 27 DNA fragments were methylated in the cell lines and GECs of *HP*-infected gerbils, but not in any GECs of gerbils without infection (Table 1; Fig. 1). The others were methylated only in the cell lines or methylated even in GECs of gerbils without infection.

Methylation in primary gastric cancers was analyzed for three randomly selected CGIs (HE6, SA9, and SB5). The methylation levels of HE6 and SB5 in eight primary cancer samples were similar to or below the mean methylation levels in GECs with *HP* infection for 50 weeks. In contrast, the methylation level of SA9 in most cancer samples was 2.1- to 19.1-fold higher than the mean methylation level in GECs from *HP*-infected gerbils (Supplementary Fig. S2). These results suggested that *HP* infection induced aberrant methylation of multiple but specific CGIs in gerbil GECs, and that methylation of some of these CGIs was associated with growth advantage of the cells.

Methylation of the corresponding CGIs in human samples. To examine whether or not these CGIs are also methylated in humans by *HP* infection, conserved regions of the

Published OnlineFirst February 2, 2010; DOI: 10.1158/0008-5472.CAN-09-2755

10 gerbil CGIs in humans were searched for. Eight of the 10 CGIs were found to be conserved between gerbils and humans (marked in Table 1), and five were located in the vicinities of genes (Fig. 2A, left). When the methylation levels of these five CGIs were quantified in human gastric mucosal biopsies, all of them had 5- to 48-fold higher methylation levels in individuals with *HP* infection ($n = 10$) than in those without ($n = 10$; right). Their methylation levels had close correlation with each other (correlation coefficient = 0.70–0.88; Supplementary Table S3).

The methylation levels of the five CGIs were then analyzed in primary human gastric cancers. *NTRK2, GPR37, NOL4,* and *NPTX2* had methylation in seven, three, four, and five, respectively, of 14 cancers analyzed, using the average methylation level of mucosal biopsies of *HP*-infected healthy volunteers as a threshold. There was no case with methylation of *RNF152* (Fig. 2B). These results showed that some of these CGIs were also methylated in human gastric cancers.

Induction of DNA methylation by chronic* HP *infection. Using the 10 CGIs isolated by MS-RDA, the effect of *HP* infection on methylation induction was analyzed at 1, 5, 10, and 50 weeks after *HP* infection (Fig. 3A). The methylation levels of HG2, SB5, and SD2 started to increase at 5 weeks after infection. At 10 weeks, CGIs other than SE3 and SH6 showed significantly higher methylation levels than those of the noninfected gerbils (3.2- to 85.0-fold). At 50 weeks, all the CGIs showed significantly higher methylation levels (14.3- to 215-fold; Fig. 3B; Supplementary Fig. S3). These results suggested that chronic *HP* infection, not acute *HP* infection, was responsible for methylation induction.

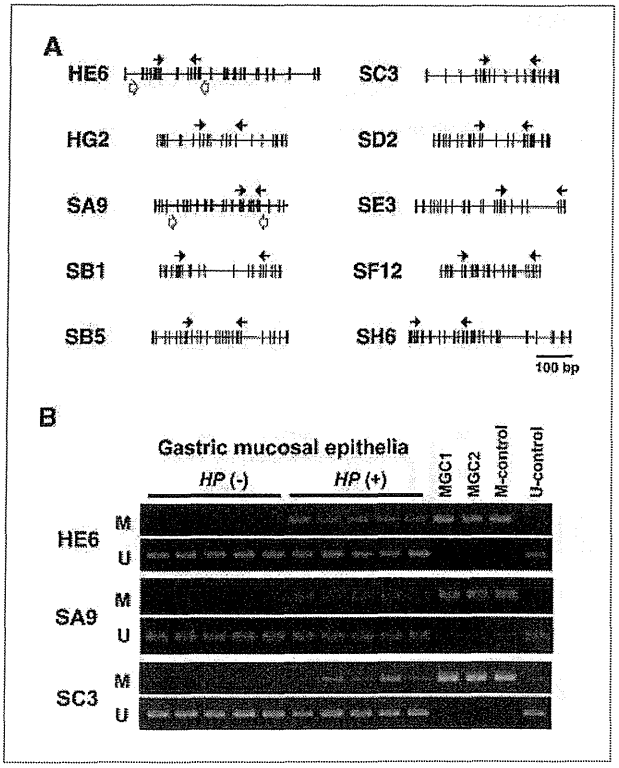

Figure 1. Isolation of CGIs that were aberrantly methylated in gerbil gastric cancers and GECs. A, a CpG map of the fragment isolated by MS-RDA. Vertical lines, individual CpG sites; arrows, positions of MSP primers; open arrows (HE6 and SA9), positions of bisulfite sequencing primers. B, representative results of MSP analyses in GECs from gerbils with and without *HP* infection for 50 wk and gastric cancer cell lines. M, MSP using a primer pair specific to methylated DNA; U, MSP using a primer pair specific to unmethylated DNA; M-control, genomic DNA treated with *SssI* methylase; U-control, DNA amplified with GenomiPhi.

The presence of dense methylation (methylation of a majority of CpG sites on a single DNA molecule) was confirmed by bisulfite sequencing of HE6 and SA9 in GECs of two gerbils with *HP* infection and two without. Densely methylated DNA molecules were detected only in *HP*-infected gerbils (Fig. 3C). The vast majority of DNA molecules were either largely unmethylated or largely methylated, and the fraction of methylated DNA molecules was in accordance with methylation levels measured by qMSP. The methylation levels of the 10 CGIs closely correlated with each other (average correlation coefficient = 0.87; range 0.70–0.95; Fig. 3D; Supplementary Table S4).

Decrease in methylation levels after* HP *eradication. *HP* was eradicated at 50 weeks after infection, and the methylation levels of the 10 CGIs were measured in GECs of the gerbils before and 1, 10, and 20 weeks after the eradication (Fig. 3A). Complete absence of *HP* was confirmed by PCR of *HP* genomic DNA (Fig. 4C). At 1 week after eradication, no decrease in methylation was observed (Fig. 3B; Supplementary Fig. S3). At 10 weeks after eradication, in contrast, the methylation levels of the 10 CGIs decreased to 9% to 32% of those before the eradication (significant for 9 of the 10 CGIs, except for SH6). An additional 10 weeks (20 weeks after eradication) did not lead to a further decrease in methylation levels. Importantly, the methylation levels after the decrease due to eradication were still significantly ($P < 0.01$ for two CGIs, and $P < 0.05$ for seven CGIs) higher than those in gerbils without any *HP* infection in their life.

Close association between methylation induction and inflammation, and not* HP *itself. *HP* infection is known to induce severe inflammation in gastric mucosae in gerbils, as in humans. Histologic analysis revealed that infiltration of polymorphonuclear cells and mononuclear cells started at 5 to 10 weeks after *HP* infection, and it became severe at 50 weeks (Fig. 4A; Supplementary Fig. S4). After eradication, a decrease in infiltration was not clear at 1 week, but was marked by 10 and 20 weeks (Fig. 4A). These histologic findings were paralleled by expression of inflammatory cell markers [*Cd3g, Cd14, Ela2,* and *Ms4a1* (*Cd20*) for T cell, macrophage, neutrophil, and B cell, respectively] in gastric tissues containing both mucosal and submucosal layers (Fig. 4B). Although *Ms4a1* expression decreased after eradication, gerbils without eradication (continuous infection) also showed a similar decrease, indicating that the decrease in *Ms4a1* expression (B-cell infiltration) was independent of *HP* eradication.

To explore the components of inflammation associated with methylation induction, the expression of inflammation-related genes [*Cox2, Cxcl2* (*MIP-2*), *Ifng, Il1b, Il2, Il4,*

Published OnlineFirst February 2, 2010; DOI: 10.1158/0008-5472.CAN-09-2755

Il6, Il7, Nos2 (*iNos*), and *Tnf* (*Tnf-α*)] was also quantified (Fig. 4B). A marked increase after *HP* infection and a decrease after eradication were observed for *Cxcl2, Il1b, Nos2,* and *Tnf,* paralleling inflammatory cell markers (Fig. 4B). The *Cox2, Ifng, Il2, Il4,* and *Il6* expression did not parallel the methylation levels after *HP* eradication, and the *Il7* expression showed a paradoxical increase compared with the group of continuous infection (Fig. 4B). Regarding the amount of *HP* in gastric mucosae, it had no association with methylation levels (Fig. 4C).

There remained a possibility that inflammatory cells had methylation of the CGIs analyzed, and that their contamination into GECs led to an apparent increase in methylation levels. To exclude this possibility, we analyzed the methylation levels of the 10 CGIs in DNA extracted from the whole blood of *HP*-infected gerbils. With the exception of SB1 and SB5, which showed relatively high methylation levels in the blood, 8 of the 10 CGIs showed almost no methylation (Supplementary Fig. S5). This excluded the possibility that methylation detected in the GECs was due to methylation in inflammatory cells contaminating the GECs.

Suppression of methylation induction by suppression of inflammation. To conclude that inflammation is indispensable for methylation induction, we suppressed *HP*-induced inflammation by administration of CsA, which blocks T-cell activation through inhibition of the calcineurin signal

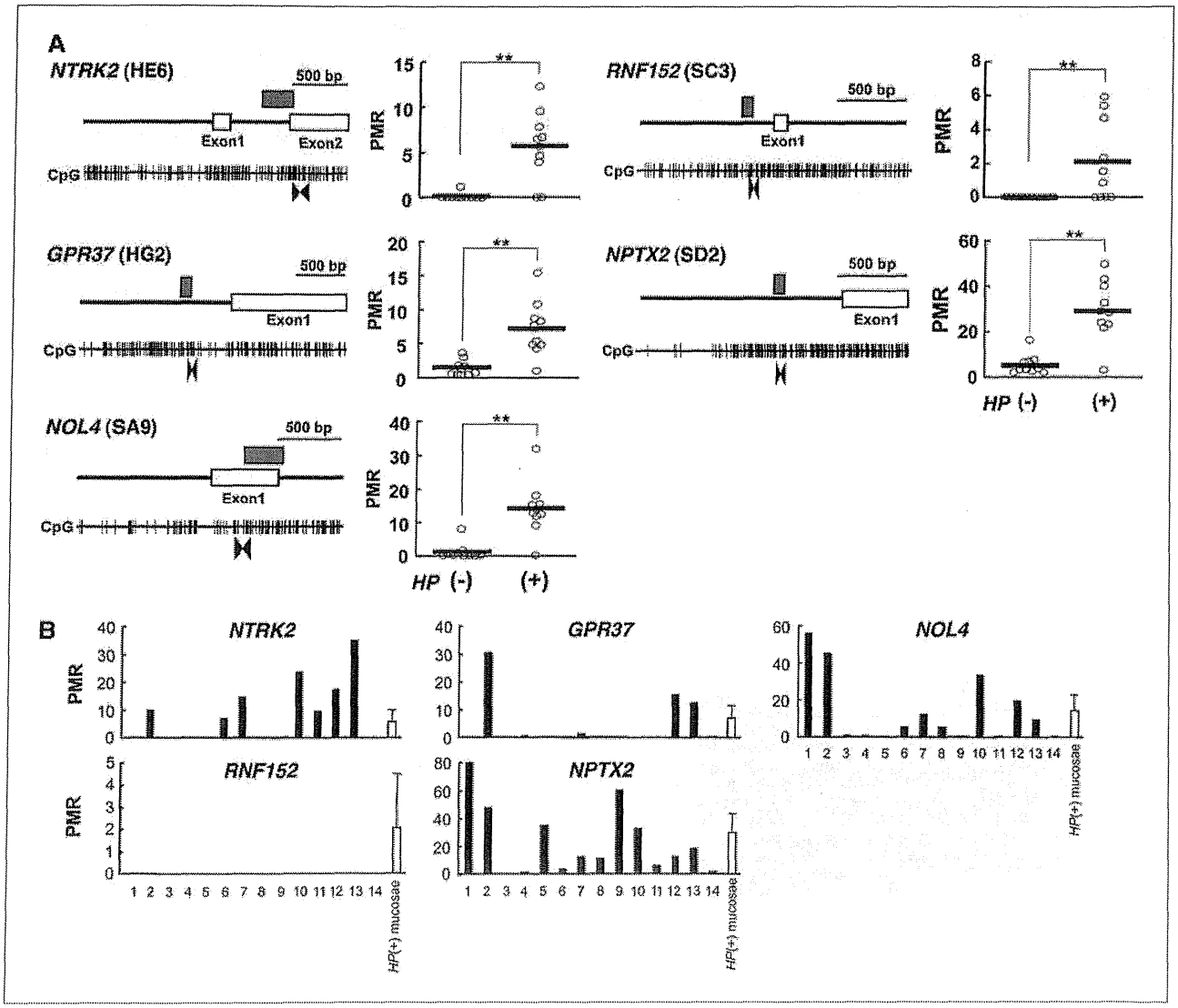

Figure 2. Methylation of homologous regions in human gastric mucosae. A, methylation levels in human gastric mucosal biopsies. Left, genomic structures and the regions analyzed by qMSP. Vertical lines, individual CpG sites; gray box, regions with homology between gerbil and man; open boxes, exons; faced arrowheads, positions of primers for qMSP. Right, result of qMSP analyses. Methylation levels were quantified in 10 healthy volunteers without *HP* infection and 10 with *HP* infection. Bold horizontal bars, average. **, $P < 0.01$. B, methylation levels in primary gastric cancers. Fourteen primary gastric cancer samples and a pool of 10 mucosal biopsies of *HP*-infected healthy volunteers were analyzed. For the gastric mucosae, their mean methylation level and SD are shown. PMR, percentage of the methylated reference.

Published OnlineFirst February 2, 2010; DOI: 10.1158/0008-5472.CAN-09-2755

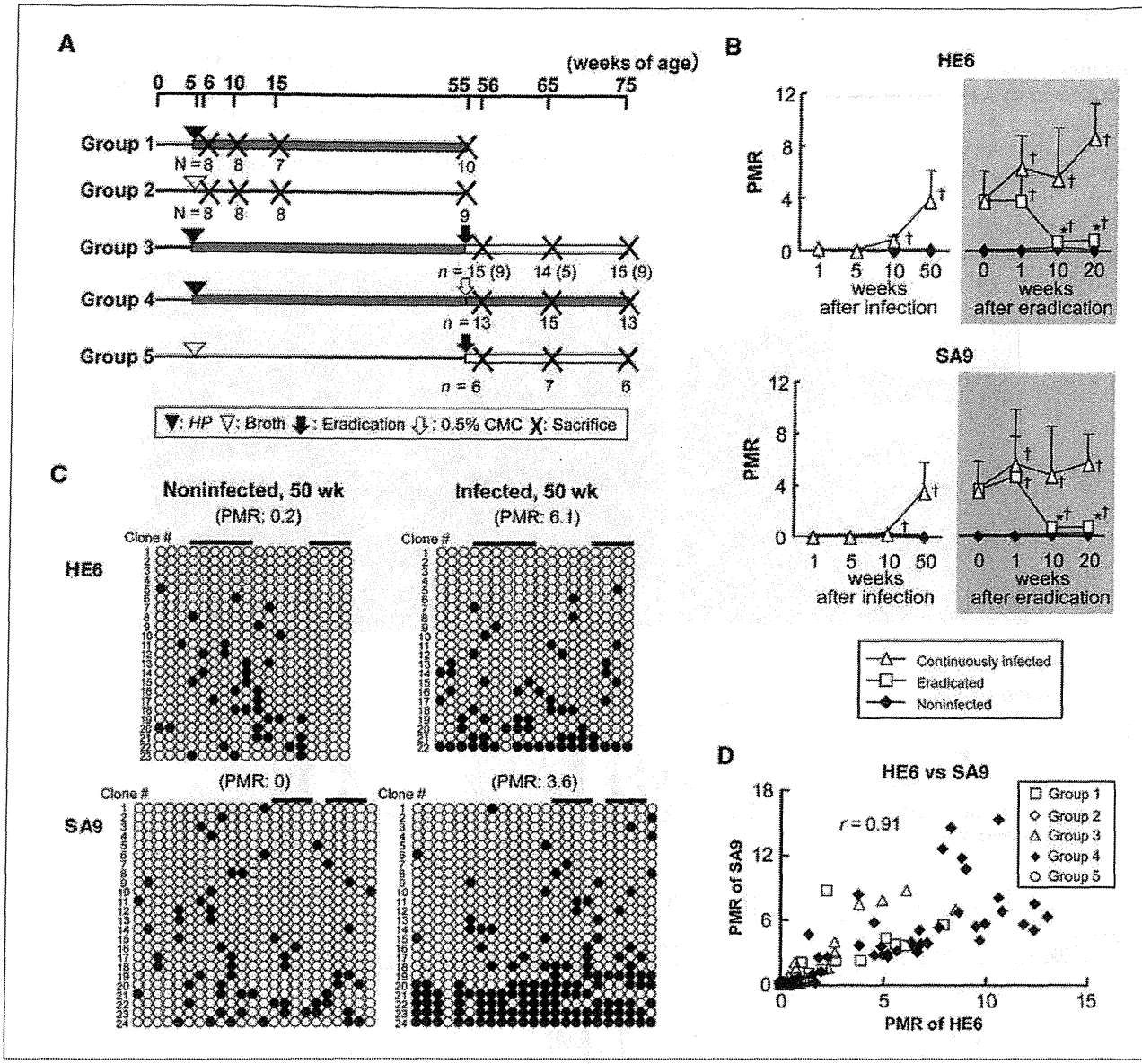

Figure 3. Temporal profiles of DNA methylation levels after *HP* infection and its eradication. A, experimental design for *HP* infection and eradication. The numbers of gerbils that were successfully eradicated of *HP* are indicated in parentheses. B, temporal profiles of methylation levels. Methylation levels are shown as mean + SD. †, $P < 0.05$, compared with noninfected gerbils; *, $P < 0.05$, compared with the methylation level before the eradication. C, the presence of dense methylation in the GECs of gerbils with *HP* infection. Bisulfite sequencing of HE6 and SA9 was done in GECs of a gerbil infected with *HP* for 50 wk and an age-matched control gerbil. The fractions of clones with dense methylation were in accordance with methylation levels (percentages of the methylated reference given in parentheses). Bars, CpG sites on which qMSP primers were designed. Similar patterns were observed for another pair of noninfected and infected gerbils (data not shown). D, scattered plot of methylation levels of HE6 versus those of SA9. The values of all 149 gerbils whose methylation was analyzed in this study were plotted. *r*, correlation coefficient.

(ref. 28; Fig. 5A). Macroscopically, administration of CsA to *HP*-infected gerbils markedly suppressed erosion and the formation of nodules. Histologically, it suppressed induction of hyperplasia almost completely, but infiltration of mononuclear and polymorphonuclear cells remained (Fig. 5B). Importantly, the number of *HP* colonized in the stomach was not affected by the CsA treatment (Supplementary Fig. S6). The expression levels of inflammatory cell markers (*Cd3g*, *Cd14*, and *Ela2*) were not reduced, indicating that the number of inflammatory cells normalized against other cells was not affected. However, the expression of three inflammation-related genes (*Cxcl2*, *Il1b*, and *Nos2*), whose expression paralleled methylation induction in the temporal analysis, was significantly reduced by the CsA treatment (Fig. 5C).

The DNA methylation levels of the 10 CGIs were markedly reduced in GECs of CsA-treated gerbils (0% to 28% of methylation levels of GECs from *HP*-infected gerbil without the